Progress in Oceanography 141 (2016) 239–258

Contents lists available at ScienceDirect

Progress in Oceanography

journal homepage: www.elsevier.com/locate/pocean

# The current system east of the Ryukyu Islands as revealed by a global ocean reanalysis

Prasad G. Thoppil [a,*], E. Joseph Metzger [a], Harley E. Hurlburt [b], Ole Martin Smedstad [c], Hiroshi Ichikawa [d,1]

[a] Open Ocean Processes and Predictions, Naval Research Laboratory, Stennis Space Center, MS 39529, USA
[b] Center for Ocean-Atmospheric Prediction Studies, Florida State University, Tallahassee, FL 32306, USA
[c] Vencore, Stennis Space Center, MS 39529, USA
[d] Japan Agency for Marine-Earth Science and Technology, Kanagawa 237-0061, Japan

ARTICLE INFO

*Article history:*
Received 4 May 2015
Received in revised form 1 December 2015
Accepted 30 December 2015
Available online 6 January 2016

ABSTRACT

The structure and variability of the Ryukyu Current System (RCS), which forms the western boundary current along the eastern slope of the Ryukyu Islands, are studied using results from a 32-layer, 1/12.5° global HYbrid Coordinate Ocean Model (HYCOM) and Navy Coupled Ocean Data Assimilation (NCODA) reanalysis for the period 1993–2012. It is confirmed that the reanalysis realistically reproduces salient features of the observed currents at three sections southeast of Miyakojima, Okinawa and Amami-Ohshima. The mean velocity sections show well-developed subsurface velocity maxima between 700 and 900 m. The current core southeast of Amami-Ohshima shows year-to-year variations with cyclonic (anticyclonic) circulation east of Amami-Ohshima generating weak (strong) velocity cores. Interaction of the RCS with an anticyclonic eddy often produces a two-core velocity structure, with a surface core in the upper 300 m and a deeper core near 700–900 m. The horizontal structure of the RCS at 15 m depth shows a well-developed northeastward current northeast of Okinawa, which is partly fed by the southwestward extension of the anticyclonic recirculation gyre. The RCS forms a continuous northeastward current from Miyakojima to Amami-Ohshima below 500 m with shoreward intensification. The circulation at 2000 m shows a seasonal flow reversal, which is northeastward from December to June and southwestward from August to October with July and November being the transition months. The volume transports across these three sections have respective mean values of 0.6, 6.2 and 12.4 Sv ($1\ \mathrm{Sv} \equiv 10^6\ \mathrm{m^3\ s^{-1}}$) and standard deviations of 10.2, 7.1 and 11.3 Sv. They have dominant seasonal variations with the maximum in winter and spring and the minimum in summer. The interannual variation of the transport anomaly, which co-varies with the RCS core, results from westward propagating mesoscale eddies arriving from the Pacific interior.

Published by Elsevier Ltd.

## 1. Introduction

The structure and variability of the Kuroshio in the East China Sea (ECS) from east of Taiwan to Tokara Strait (Fig. 1) have been the focus of several studies (e.g., Johns et al., 2001; Zhang et al., 2001; Feng et al., 2000; Andres et al., 2008). The large difference between Kuroshio volume transports in the ECS and those south of the central Japan points to the existence of a northeastward current southeast of the Ryukyu Islands (Worthington and Kawai, 1972; Nitani, 1972), known as the Ryukyu Current System (RCS). These two western boundary currents, which are mostly separated by the long chain of Ryukyu Islands, have distinct characteristics while both of them are flowing northeastward. The RCS is weaker, deeper, and relatively unstable compared to the much stronger, shallower and more stable Kuroshio in the ECS. Unlike the Kuroshio, which is constrained by sill depths and the steep bathymetry along the continental shelf break in the ECS, the RCS is directly influenced by mesoscale eddies from the east. The interaction of these currents through the Kerama Gap, with a sill depth of ~1000 m, appears to influence the Kuroshio transport variability in the ECS by interacting with eddies and plays an important role in exchanging water masses between the ECS and the western Pacific (Andres et al., 2008; Na et al., 2014; Yu et al., 2015). After exiting the ECS through Tokara Strait, the Kuroshio joins the RCS, thereby increasing the Kuroshio volume transport. For example, Ichikawa and Beardsley (1993), Lee et al. (2001) and Zhu et al. (2006) reported the RCS contribution to be 11.4, 12 and 13 Sv, respectively. The RCS northeast of Okinawa is also at least partially fed by the anticyclonic recirculation gyre that extends southwestward from Japan (Nakamura et al., 2007). A unique feature that

* Corresponding author. Tel.: +1 228 688 5500; fax: +1 228 688 4759.
*E-mail address:* prasad.thoppil@nrlssc.navy.mil (P.G. Thoppil).
[1] Present address: Anjindai, Yokosuka, Kanagawa 238-0048, Japan.

http://dx.doi.org/10.1016/j.pocean.2015.12.013
0079-6611/Published by Elsevier Ltd.

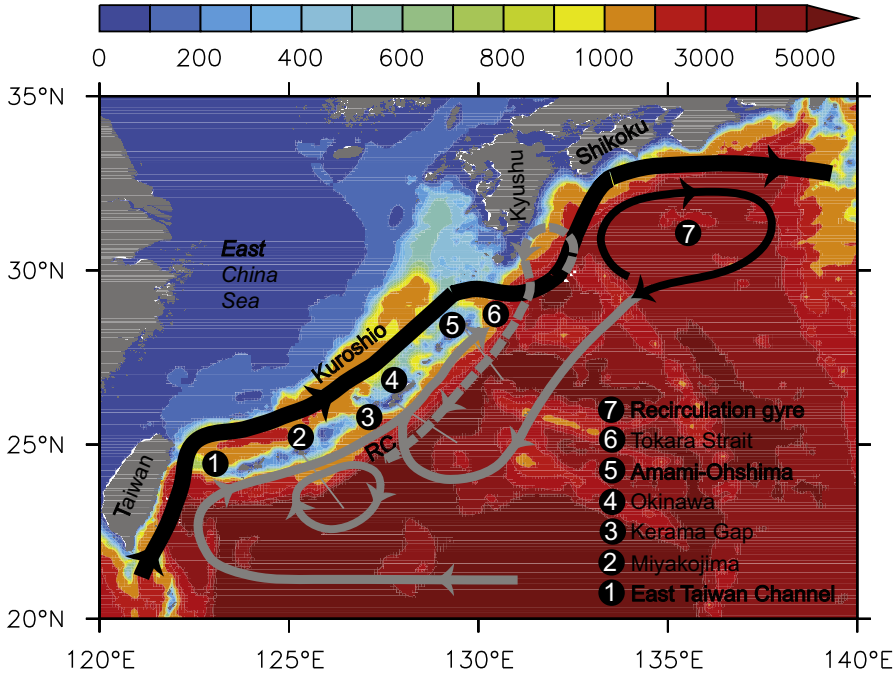


**Fig. 1.** Schematic of the circulation in the northwestern Pacific Ocean, including east of the Ryukyu Islands. The three sections southeast of Miyakojima, Okinawa, and Amami-Ohshima (ordered from south to north) discussed in the paper are indicated by grey lines. On the basis of this and previous studies, we reconstructed the Ryukyu Current System (RCS), which is shown by the solid grey arrow. The dashed grey line shows the quasi-steady southwestward current below ~2000 m. The bottom topography (in meters) is shown in color.

clearly differentiates the RCS from the Kuroshio is the subsurface intensification of the RCS northeast of Okinawa due to the shallow sill depth at the Kuroshio outflow from the ECS.

Using current meter observations and satellite altimeter data from January 1998 to July 2002, Ichikawa et al. (2004) showed evidence for a persistent northeastward current southeast of Amami-Ohshima with a subsurface velocity core of 23 cm $s^{-1}$ at 600 m. Zhu et al. (2010) reported a mean absolute geostrophic velocity of 24.6 cm $s^{-1}$ at 326 dbar southeast of Amami-Ohshima from inverse calculations using 16 repeated hydrographic sections from April 2003 to June 2007. They also indicated a stronger Ryukyu current above 700 m in autumn. Limited observations southeast of Okinawa indicate a northeastward current with occasional weak current cores (Yuan et al., 1994; Liu and Yuan, 2000; Zhu et al., 2004, 2008). The mean geostrophic velocity derived from a Pressure Inverted Echo Sounder (PIES) during November 2000–August 2001 (270 days) southeast of Okinawa is 20 cm $s^{-1}$, with a northeastward (southwestward) currents up to 60 cm $s^{-1}$ (15 cm $s^{-1}$) when anticyclonic (cyclonic) eddies were present (Zhu et al., 2003). The northward intensification of the RCS northeast of Okinawa has also been reported in some studies (e.g., You and Yoon, 2004; Ichikawa et al., 2004; Nagano et al., 2007, 2008; Zhu et al., 2008). Zhu et al. (2005) suggested a connectivity of the RCS southeast of Amami-Ohshima to that southeast of Okinawa during their short observational period (2–10 December 2000). The mean structure of the RCS southeast of Okinawa and Amami-Ohshima has been investigated from geostrophic velocity derived using an inverse method and hydrographic observations during 26 May–7 June, 14–21 September and 17–28 October 2002 (Nagano et al., 2007, 2008; Zhu et al., 2008). As pointed out subsequently by Zhu et al. (2008) and Nagano et al. (2008), their geostrophic velocity was strongly constrained by the choice of a shallow reference depth of 100 dbar. Nevertheless, Nagano et al. (2007) found large variability in the depth and magnitude of the velocity core during these periods. The geostrophic velocity relative to a 2000 dbar reference level showed a maximum northeastward current of ~60 cm $s^{-1}$ at 250 m southeast of Amami-Ohshima, based on the October data (Zhu et al., 2008, their Fig. 2). A much weaker northeastward current core of 20 cm $s^{-1}$ was reported along the Okinawa section by Zhu et al. (2008, their Fig. 3).

The volume transports of the RCS southeast of Amami-Ohshima and Okinawa vary widely among the several studies. Ichikawa et al. (2004) estimated a 4.5-year mean northeastward volume transport of 16 Sv in the upper 1500 m southeast of Amami-Ohshima, employing absolute geostrophic currents derived from current meter observations and satellite altimeter data. Zhu et al. (2010) indicated 14 Sv from an inverse method using 16 hydrographic sections during April 2003–June 2007 southeast of Amami-Ohshima. The geostrophic volume transport relative to the 2000 dbar level southeast of Okinawa from the PIES during November 2000–August 2001 (270 days), found by Zhu et al. (2003), is 6.1 Sv. By correlating the transport values during this period with the sea surface height anomaly difference (SSHAD) and tide gauge data, using the method of Imawaki et al. (2001), Zhu et al. (2004) derived a 9-year (1992–2001) mean transport of 4.5 Sv with a standard deviation of 5.5 Sv. An inverse technique used with the hydrographic data collected during 2–10 December 2000 (Zhu et al., 2005), produced ~15 Sv of volume transport in both the regions southeast of Okinawa and Amami-Ohshima. Using a modified inverse method, Liu and Yuan (2000) estimated the volume transports southeast of Okinawa during three cruises in 1998 to be 3, 8 and 10 Sv.

The conclusions drawn from the preceding studies, however, suffer from several problems. First, the temporal and spatial distribution of observations (hydrographic and current meter) used to estimate the mean velocity and volume transport are limited, making representativeness of estimated means a serious issue, especially in the presence of mesoscale eddies. Mesoscale eddies from the interior ocean (~100 days) are a significant source of variability in these regions, which can yield substantial aliasing in individual hydrographic surveys or short-term current meter observations (e.g. Liu and Yuan, 2000; Zhu et al., 2000; Zhu et al., 2008, 2010). The second issue is the uncertainty associated with the derivation of geostrophic velocity using hydrographic observations, PIES, or inverse technique and the choice of a level of no motion. Thirdly,

the accuracy of volume transports estimated from the SSHAD (Zhu et al., 2004), is also an issue. The absence of a strong lateral SSH gradient associated with the RCS in the satellite altimeter data makes this method less attractive, although it has been used for the estimation of Kuroshio volume transport south of Japan (e.g. Imawaki et al., 2001).

There have been only a few numerical modeling studies focused on the RCS. While non-assimilative ocean models are useful in exploring the dynamical processes involving the RCS vertical structure (e.g. You and Yoon, 2004; Nakamura et al., 2007; You et al., 2009), they tend to misrepresent the strength and depth of current core. In a Pacific Ocean circulation model, You et al. (2009) reproduced the RCS with a subsurface core at 500–600 m, although the core velocity east of Amami-Ohshima (35 cm $s^{-1}$) is much stronger than observed (23 cm $s^{-1}$). Nakamura et al. (2007) indicated a current core in their sections southeast of Okinawa and Amami-Ohshima that is deeper than ~1000 m. Using an operational ocean data assimilation system for the Kuroshio, Kamachi et al. (2004) briefly discussed the horizontal structure and volume transport of the RCS found in a 9-year reanalysis (1993–2001) and suggested a gradual increase in volume transport from 5–10 Sv southeast of Okinawa to 20 Sv east of Amami-Ohshima. They also point out that the year-to-year variation of the RCS core southeast of Amami-Ohshima is not adequately reproduced in the reanalysis.

The key to a better understanding of the structure and variability of the RCS using an ocean model depends on how well the model represents the ocean dynamics that influence the RCS. First, the RCS structure southeast of Amami-Ohshima is influenced in part by the location of a large anticyclonic recirculation gyre associated with the Kuroshio. Accurate representation of this gyre in non-assimilative models has been a challenge due to its non-linearity. Second, westward propagating mesoscale eddies from the interior ocean have a large influence on the variation of volume transport southeast of the Ryukyu Islands. The characteristics of eddies in non-assimilative models tend to be different from observations. The data-assimilative models have shown significant ability to reproduce the ocean state, although they are less suitable for exploring the dynamical processes involving the RCS. The data-assimilation provides a contemporaneous ocean state that is suitable not only for the detailed study of structure and variability of the RCS but also can be used to fill in spatial and temporal gaps in the observations. This study aims to investigate the continuity of the RCS using 20 years of the output from a data assimilative global HYbrid Coordinate Ocean Model (HYCOM) hindcast, hereinafter referred to as reanalysis, and has two objectives. The first is to validate the reanalysis over the period 1993–2012 using independent velocity observations in the regions east of the Ryukyu Islands, specifically Miyakojima, Okinawa and Amami-Ohshima. The second objective is to elucidate the annual and interannual variability of the RCS velocity structure across both space and time, not covered by the current meter observations, with a major focus on the subsurface velocity core.

The remainder of this paper is organized as follows. We briefly introduce the model set-up, data, and assimilation system in Section 2. A more detailed description can be found in Cummings and Smedstad (2013). The structure of the RCS from the reanalysis is compared to independent observations that include vertical cross-sections of velocity and time-series of velocity vectors across sections southeast of Amami-Ohshima, Okinawa and Miyakojima in Section 3.1. The mean structure and variability of the RCS from the reanalysis and observations are presented in Section 3.2. An important feature of the RCS is the existence of a subsurface velocity maximum at intermediate depths. Its annual and interannual variability along these sections are presented in Section 3.3. This is followed by the presentation of annual and interannual variability of volume transport in Section 3.4. The important contributions of mesoscale eddies in the variabilities of core velocity and volume transport are discussed using the reanalysis sea surface height anomalies (SSHA). Major findings are summarized in Section 4.

## 2. Global HYCOM/NCODA

Employing global HYCOM as the ocean component and the Navy Coupled Ocean Data Assimilation (NCODA) (Metzger et al., 2014), hereafter referred to as HYCOM/NCODA, the reanalysis is performed from 1993 to 2012. Global HYCOM has horizontal resolution of 0.08° (1/12.5° or ~9 km near the equator, ~7 km at mid-latitudes and ~3.5 km near the North Pole), which makes it eddy-resolving and able to capture mesoscale variability. The HYCOM grid is uniform cylindrical from 78.64–66°S, and a Mercator projection from 66°S to 47°N. North of 47°N it employs an Arctic dipole grid, where the poles are shifted over land to avoid a singularity at the North Pole. This version employs 32 hybrid vertical coordinate surfaces with potential density referenced to 2000 m. HYCOM uses the K-Profile Parameterization vertical mixing. A more complete description of HYCOM physics can be found in Bleck (2002). Several HYCOM/NCODA validation tests, using independent observations and a variety of metrics have been performed for various regions (Metzger et al., 2008, 2010). The atmospheric forcing for the ocean model came from the National Centers for Environmental Prediction (NCEP) Climate Forecast System Reanalysis (CFSR, Saha et al., 2010). CFSR is the result of an effort to generate a uniform, continuous, and best estimate record of the state of the atmosphere by assimilating observations from many data sources. The CFSR was run from 1979 through the present with a horizontal resolution of 0.3125°, and provided hourly output for the global HYCOM/NCODA reanalysis.

NCODA is a fully 3D, multivariate, variational ocean data assimilation scheme (Cummings and Smedstad, 2013). The three-dimensional ocean analysis variables include temperature, salinity, geopotential, and vector velocity components, all of which are analyzed simultaneously. NCODA can be run in stand-alone mode, but here it is cycled with HYCOM to provide updated initial conditions for the next model forecast in a sequential incremental update cycle. Corrections to the HYCOM forecast are based on all observations that have become available since the last analysis. These include surface observations from satellites, such as altimeter sea surface height (SSH) anomalies, sea surface temperature (SST), and sea ice concentration, plus in-situ SST observations from ships and buoys as well as temperature and salinity profile data from XBTs, CTDs, gliders and Argo floats. See Table 13.1 in Cummings and Smedstad (2013) for a more complete list, but new observational data types are routinely added. By combining the various observational data types via data assimilation and using the dynamical interpolation skill of the model, the 3D ocean environment can be more accurately nowcast and forecast.

The HYCOM/NCODA system is run as follows: a single daily update cycle starts with the NCODA analysis at 18Z GMT (Greenwich Mean Time) using the HYCOM 24-h forecast as a first guess and with the analysis window for altimeter data spanning ±36 h, for profile data spanning −12 days to +12 h, and for all other observations spanning ±12 h. Then HYCOM is run for 24 model hours with the NCODA incremental analysis update (Bloom et al., 1996) applied to the ocean model over the first six hours. Thus at 00Z HYCOM has fully assimilated all the observational data.

## 3. Results

### 3.1. Velocity structure east of the Ryukyu Islands

In this section, we use both direct comparisons and statistical methods to determine how well the reanalysis reproduces the

RCS with a special focus on three locations, Amami-Ohshima, Okinawa and Miyakojima. In the following subsections, the structure of RCS from the reanalysis for each of these sections is compared to independent observations that include vertical cross-sections of velocity (both temporal mean and snapshots) and time-series of velocity vectors. We also used geostrophic velocity derived either from direct or indirect methods by previous studies. Comparisons are limited to the observation period. Beyond model-data comparisons, we use the reanalysis to identify the spatial continuity of the RCS from east of Taiwan to south of Japan and temporal variability of the RCS on seasonal to interannual time scales.

*3.1.1. Amami-Ohshima*

Using a combination of current meter observations and satellite altimeter data, Ichikawa et al. (2004) estimated the mean velocity structure southeast of Amami-Ohshima during December 1998–July 2002. The current meter data indicated a northeastward current with a subsurface velocity maximum of 23 cm $s^{-1}$ at around 600 m depth, located over the slope north of 27.6°N (their Fig. 8, reproduced in Fig. 2j). The mean velocity from the reanalysis during the period of current meter observations (December 1998–July 2002) shows a similar northeastward current with a subsurface maximum of 16 cm $s^{-1}$ at 750 m near 27.7°N (Fig. 2e), while it is weaker than the observations (Fig. 2j) by 30%. The differences in velocity core magnitude and depth between the reanalysis and observations should be viewed in light of the methodology used to compute the observed current. Ichikawa et al. (2004) demonstrated this point in their Fig. 9, where they compared absolute geostrophic currents derived using temperature observations with current meter data. The velocity core from current meter observations occurred at 700 m with a velocity of 15 cm $s^{-1}$, while that derived from the geostrophic method was 25 cm $s^{-1}$. They attributed the difference in velocity core position to the current meter observations being low-pass filtered. Furthermore, the horizontal and vertical resolution of the current meter observations were inadequate to accurately resolve the depth of the current core.

Ichikawa et al. (2004) presented vertical sections of mean velocity during each one-year mooring period: December 1998–November 1999, November 1999–November 2000, November 2000–November 2001 and November 2001–July 2002 southeast of Amami-Ohshima (their Fig. 7), which is reproduced in Fig. 2f–i and compared to corresponding velocity sections from the reanalysis in Fig. 2a–d. The reanalysis reveals the velocity core associated with the RCS in each one-year period with some year-to-year variations. The standard deviation of the core velocity at 750 m during this period is 9 cm $s^{-1}$. With the exceptions of magnitude and depth of the current core, the reanalysis generally reproduces the year-to-year variability consistent with the observations (Fig. 2f–i). The strongest core occurred in 1999 with a velocity of 20 cm $s^{-1}$ at 800 m (Fig. 2a), compared to >30 cm $s^{-1}$ at 500 m in the observations (Fig. 2f). The weakest core velocity occurred during the year 2001 with a magnitude of 14 cm $s^{-1}$, close to the observed value of 16 cm $s^{-1}$. The velocity core during this period is located slightly farther offshore (~27.7°N) than the other periods, which is consistent with the observations (27.6°N). In contrast, the core is closer onshore (27.9°N) during the 1999–2000 period and reduced in spatial extent. It should be noted that the observed velocity core is sensitive to the location of the current meters (circles), which are inadequate to resolve the current core. A southwestward current in the upper 500 m of the inshore slope area of the section demarcates the Kuroshio return flow from Tokara Strait, which falls outside the velocity sections of Ichikawa et al. (2004).

The reanalysis provides further insight into such year-to-year variations in the RCS core southeast of Amami-Ohshima. Anomalies of current vectors and speed (shaded) at 700 m relative to the December 1998–July 2002 mean for each period (Fig. 3) illustrate the impact of mesoscale eddies on the year-to-year variability. In general, the periods of strong RCS current core are associated with an anticyclonic eddy in the region southeast of Amami-Ohshima and the existence of a cyclonic eddy during periods of a weak current core. During 1998–99, the anticyclonic eddy southeast of Amami-Ohshima (indicated by a red triangle) causes the RCS to increase by 2–4 cm $s^{-1}$ (Fig. 3a). In contrast, a cyclonic eddy (indicated by a blue triangle) during 1999–2000 causes a reduction in current core velocity by 4–6 cm $s^{-1}$ (Fig. 3b). The structure of the eddies during 2000–2001 resembles those during 1999–2000, except that the eddies are further to the northeast. The cyclonic eddy (anticyclonic eddy) southeast of Amami-Ohshima during 1999–2000 (2000–2001) moves the velocity core farther onshore (offshore). It is worth noting that a stronger (weaker) current core southeast of Amami-Ohshima is accompanied by a weaker (stronger) core southeast of Okinawa during these periods.

The temporal variation of velocity vectors from the reanalysis is compared with independent moored current meter observations from Ichikawa et al. (2004) during the period December 1998–October 2002. Fig. 4a displays the velocity vectors at various depths from the observations (black) and the reanalysis (red) linearly interpolated onto the locations of observation sites. The reanalysis reproduces the observations of a predominantly northeastward current at all depths and locations. To quantify the comparisons, the squared vector correlation ($\rho_v^2$) is calculated between the observations and the reanalysis following Crosby et al. (1993) and is shown in magenta. Throughout this study we quote $\rho_v^2$, which varies between 0.0 (no correlation) and 2.0 (perfect correlation). The vector correlations ($\rho_v^2$) during each observation period show highly correlated ($\rho_v^2 > 0.31$ is statistically significant at $p < 0.0001$) reanalysis velocities during most of the period with $\rho_v^2$ ranging between 1.21 and 0.35 (Fig. 4a). The reanalysis also reproduced the low-frequency variability evident in the observations. Separated by about 72 km, it is not surprising that the flow variability across the stations S1 and S6 is generally similar regardless of depth, but with a gradual decrease in current speed south of S2 (27.76°N). Although the reanalysis velocity qualitatively agrees with the observations, there are notable differences in the current magnitude at 27.91°N (S1), where the reanalysis velocity is weaker than the observations by ~57%. The reanalysis mean current speed at S1 is ~16 cm $s^{-1}$ compared to 35 cm $s^{-1}$ in the observations. The strongest mean current (21.5 cm $s^{-1}$) among the sections is seen near 27.76°N at 654 m (S2), which indicates the subsurface core is located slightly north (~27.9°N) and shallower (~600 m) than in the observations (S1). Both the reanalysis and the observations indicate the modulation of the currents by the mesoscale eddies. For example, a northwestward current followed by a southeastward current at all latitudes during January–February 2000 is associated with a cyclonic eddy. However, southwestward currents around June 2002 observed at S1 and S2, possibly driven by a cyclonic eddy, are not reproduced by the reanalysis. There are also periods of rapid intensification such as a strong northeastward current in January 2002. Overall, in both the observations and the reanalysis, the predominant flow is toward the northeast with the intermittent intensifications.

Although the published analysis of Ichikawa et al. (2004) was limited to the moorings used in Fig. 4a, comparisons of the reanalysis with the additional current meter observations, shown in Figs. 4b and 4c, help us to validate the currents below ~1000 m, including the abyssal ocean. Except for the depths, the locations of these current meter observations are similar to Fig. 4a. The current is generally northeastward north of S3 (960–1663 m), but more variable at deeper depths farther offshore, where the current

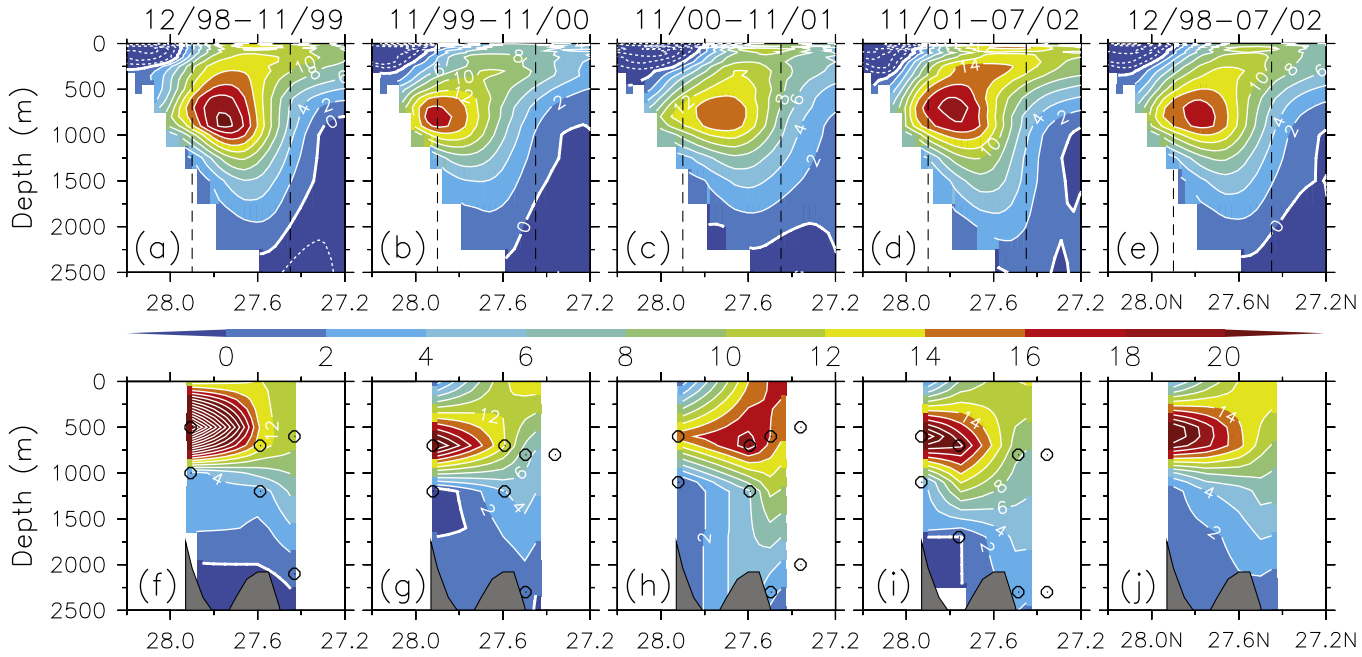


**Fig. 2.** Vertical sections of mean velocity (cm $s^{-1}$) southeast of Amami-Ohshima from the reanalysis during the current meter observation periods of Ichikawa et al. (2004) for (a) December 1998–November 1999, (b) November 1999–November 2000, (c) November 2000–November 2001, (d) November 2001–July 2002, and (e) December 1998–July 2002, and (f–j) the corresponding velocity observations reproduced from Ichikawa et al. (2004, their Figs. 7 and 8). The contour interval is 2 cm $s^{-1}$. Dashed contours indicate southwestward flow. The locations of current meter observations are marked in circles. The current core between 500 and 1000 m shows large year to year variations consistent with the observations.

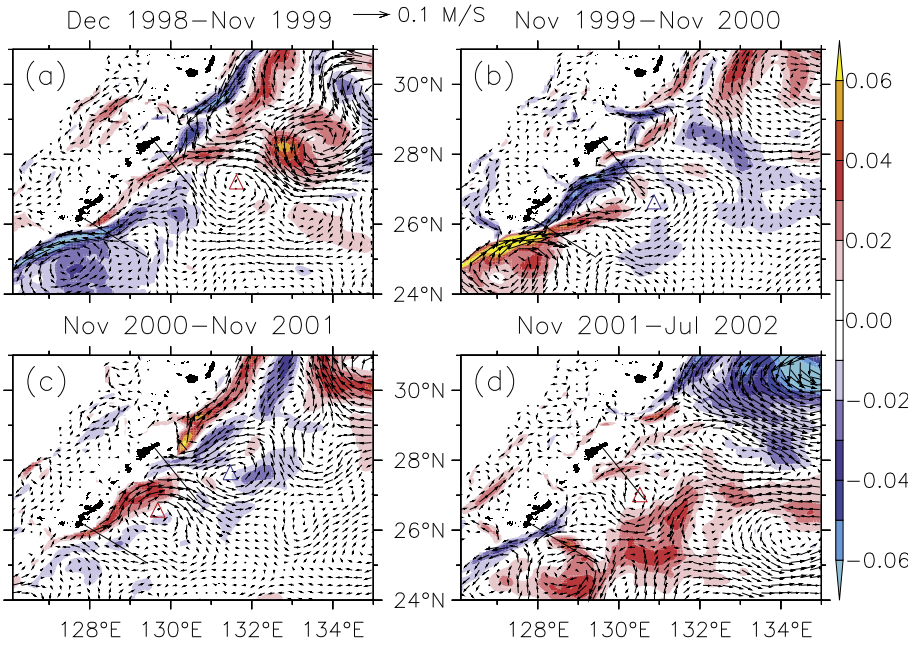


**Fig. 3.** Anomalies of velocity vectors (m $s^{-1}$) and speed (shaded) at 700 m from the reanalysis relative to the December 1998–July 2002 mean for (a) December 1998–November 1999, (b) November 1999–November 2000, (c) November 2000–November 2001, and (d) November 2001–July 2002. The center of cyclonic (anticyclonic) circulation is indicated by a blue (red) triangle. The reference vector is shown at the top.

undulates between northeast and southwest (Fig. 4b). A persistent northeastward current, evident at S3 (27.59°N), is reproduced by the reanalysis. Although there is broad agreement in the direction of currents, the strength of the currents varies widely between the reanalysis and observations. For example, the mean current in the reanalysis during 1999 at S3 is stronger than the observations by 48%, whereas it is significantly weaker during 2000 at S6 by 68%. However, those currents at deeper depths, shown in Fig. 4c, have smaller differences. Both the reanalysis and observations show the currents south of S4 oscillating between northeast and southwest with a period ranging from a few months to six months (Figs. 4b and 4c). There are two important aspects of the current variability between depths of 2000 m and 3000 m depths. The circulation at 1959 m during 2001 (S6) reveals a northeastward current from January to May 2001 and a southwestward current from June to October 2001 (Fig. 4b), similar to the circulation pattern in

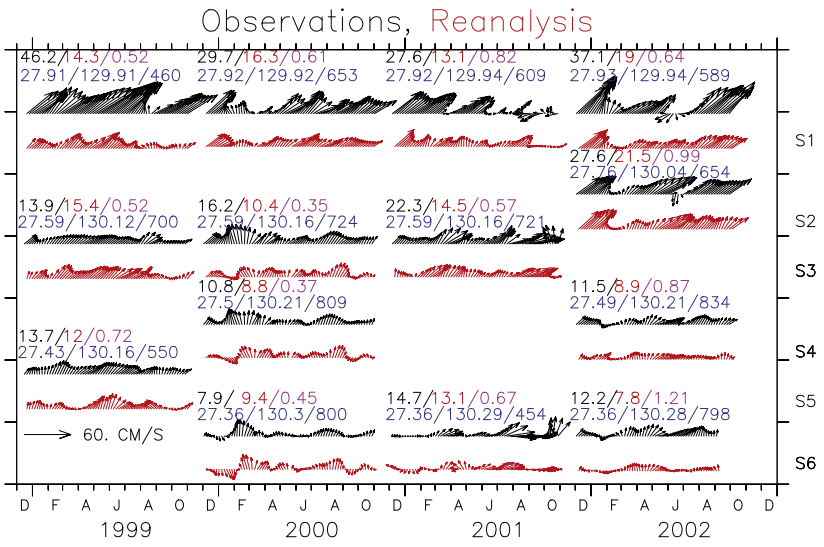


**Fig. 4a.** Comparisons of velocity vectors (cm $s^{-1}$) between the moored current meter observations (black vectors) by Ichikawa et al. (2004) and the reanalysis (red vectors) southeast of Amami-Ohshima during the period December 1998–2002. The latitude, longitude, and nominal measurement depth for each deployment are shown (blue). The average velocity during each mooring period from the observations (black) and the reanalysis (red) is also provided. The vector correlation ($\rho_v^2$) between the observations and reanalysis is computed following Crosby et al. (1993) and is shown in magenta. The squared vector correlation, $\rho_v^2$, varies between 0.0 (no correlation) and 2.0 (perfect correlation), so the correlation varies between 0.0 and $\sqrt{2}$. The sample size for each period is about 320. Velocities are shown every 5 days, after smoothing by a low-pass Lanczos filter with a 30-day period. Time series are grouped from S1 to S6 based on the approximate latitudinal location of current meter observations.

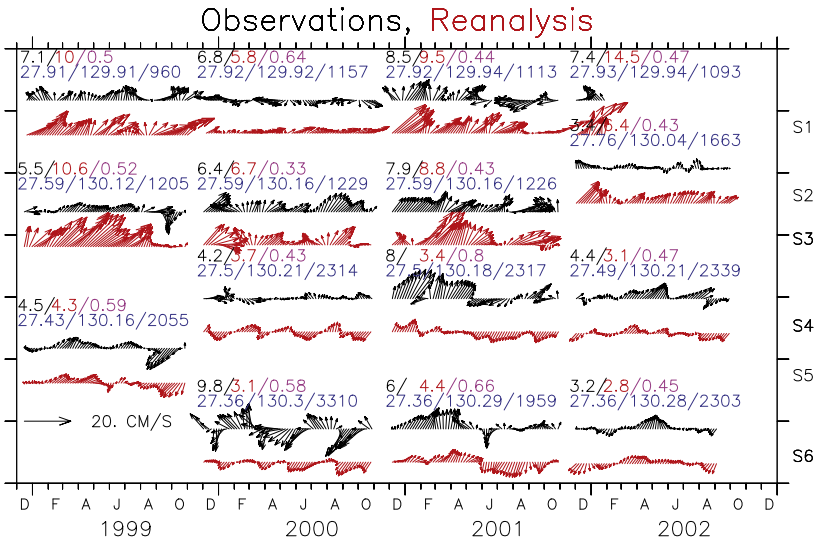


**Fig. 4b.** Same as Fig. 4a except for different depths.

the northwestern section (S4) at 2317 m. This seasonal flow reversal at 2000 m in 2001 is discussed further in Section 3.2.2.2. Another notable circulation feature is the change in direction of currents between 2000 m and 3000 m depths. The direction of the current at 2055 m from S5 is northeastward during the first half of 1999, but it is southwestward during the second half of the year (Fig. 4b). At a depth of 3060 m, the observed current at S5 in 1999 (Fig. 4c) is predominantly southwestward with a larger speed (9.5 cm $s^{-1}$) than at 2055 m depth (4.5 cm $s^{-1}$), indicating a notable bottom intensification by 110%. Similar bottom intensification of the southwestward current is also evident in 2001 (S6), where the mean speed increases to 8.9 cm $s^{-1}$ at 2964 m from 6 cm $s^{-1}$ at 1959 m (48%).

The annual mean velocity during 1999 at 2000 m and 3000 m depths from the reanalysis (Fig. 5) clearly substantiates the flow reversal and bottom intensification evident in the observations, even though the flow is not constrained by data assimilation at these depths. In fact, spatial maps depict a better representation of the bottom intensification at 3000 m seen in the observations than shown in Fig. 4c, although not at the observation location (indicated by a red triangle). The northeastward current upstream of Amami-Ohshima at 2000 m is reversed to a southwestward current at 3000 m. The southwestward current originates at ~30°N from a cyclonic eddy (indicated by a solid line box) and meets the northeastward current southeast of Amami-Ohshima (Fig. 5a). The resulting opposing currents generate an offshore branch with a part continuing southwestward. At 3000 m (Fig. 5b), the southwestward current reveals a notable bottom intensification (>5 cm $s^{-1}$) to the southeast of Amami-Ohshima. The acceleration of the current at 3000 m relative to 2000 m may

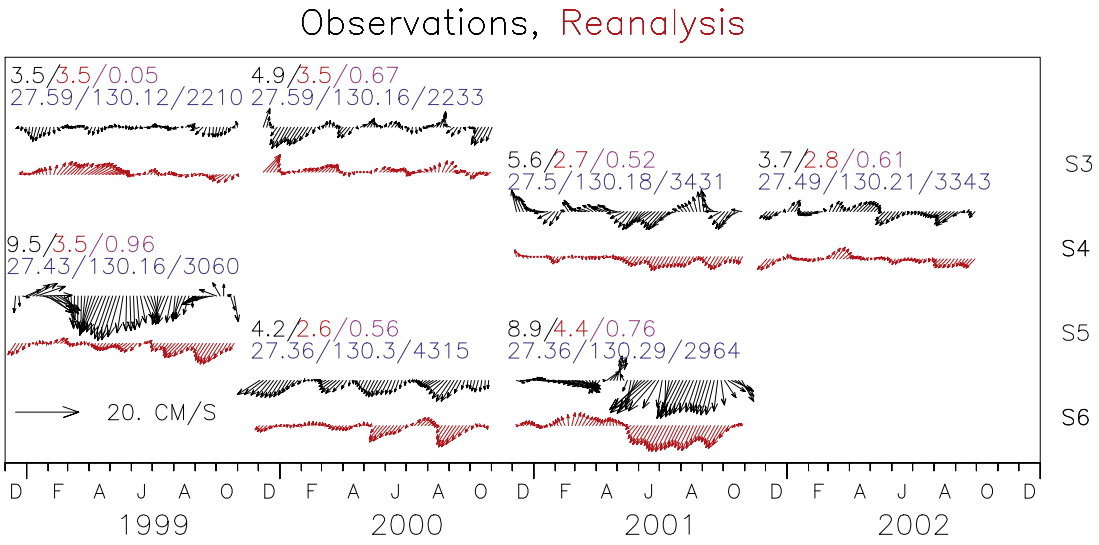


**Fig. 4c.** Same as Fig. 4a except for different depths.

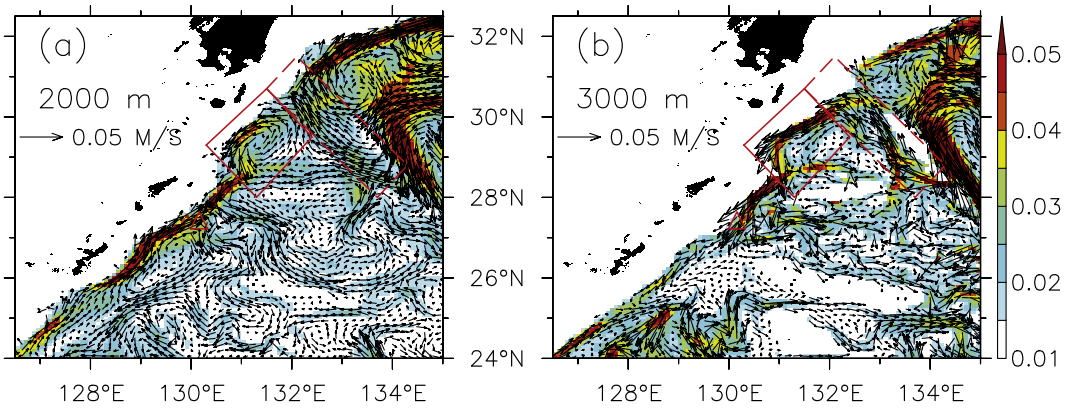


**Fig. 5.** Annual mean currents during 1999 at (a) 2000 m, and (b) 3000 m with current speed (m $s^{-1}$) shaded. Red triangle indicates the current meter locations discussed in the text. The location of a cyclonic circulation is marked with a red box and its contribution from the recirculation gyre (topographically steered) is shown in a dashed line box.

be due to the contribution from the recirculation gyre. Influenced by a bathymetric seamount (Kyushu-Palau Ridge), part of the recirculation gyre flows northwestward (indicated by a dashed line box) and feeds the southwestward current at ~30°N. This results in the bottom intensification.

### 3.1.2. Okinawa

In comparison to Amami-Ohshima, the mean structure of the RCS southeast of Okinawa has not been resolved on the basis of long-term current meter observations. Neither has the existence of a stable subsurface current core similar to that southeast of Amami-Ohshima been confirmed. Thus to validate the reanalysis, we compare the mean structure of the RCS from the reanalysis with the mean geostrophic velocity by Zhu et al. (2003) over the period November 2000 to August 2001 (270 days). The geostrophic velocity is calculated by using the vertical profiles of specific volume anomaly derived by the Gravest Empirical Mode (GEM) method from the PIES observations (see Zhu et al., 2003 for details). The mean geostrophic velocity southeast of Okinawa shows a northeastward current of 20 cm $s^{-1}$ on the onshore side in the upper 500 m with no indication of a subsurface velocity core (their Fig. 3a, reproduced in Fig. 6f). However, the mean velocity structure during the same period from the reanalysis shows a northeastward current north of 25.6°N with a well-developed current core of 20 cm $s^{-1}$ at ~900 m (Fig. 6a). These discrepancies can be attributed to the limited spatial resolution of the observations, which do not resolve the velocity core. Zhu et al. (2003) indicated the existence of at least two mesoscale eddies during the 270-day observation period, so the estimated mean current is aliased by them. Since the time interval of mesoscale eddies arriving this region is longer than 100 days, the velocity core southeast of Okinawa in the reanalysis cannot properly be validated due to the lack of long-term observations.

The impact of mesoscale eddies on the vertical structure of the RCS southeast of Okinawa has been suggested earlier (Zhu et al., 2003; Konda et al., 2005; Takikawa et al., 2005). In particular, Zhu et al. (2003) examined the vertical sections of velocity during the period of a cyclonic eddy (April 25, 2001) and an anticyclonic eddy (July 11–13, 2001), which are redrawn and shown in Fig. 6g and h for comparison with the reanalysis (Fig. 6b and e). Note that reanalysis sections are monthly means rather than snapshots. The signature of these eddies is evident in the reanalysis, except for the existence of a velocity core, with weaker (stronger) currents associated with the anticyclonic (cyclonic) eddy than the observations. It should be pointed out that the agreement is better when the reanalysis time is matched with the observations. In the reanalysis, the cyclonic eddy is confined to the upper ~600 m with a strong southwestward current on the onshore side (~40 cm $s^{-1}$) and a weak northeastward current on the offshore side (~5 cm $s^{-1}$). The eddy appears to have no effect on the structure of the core

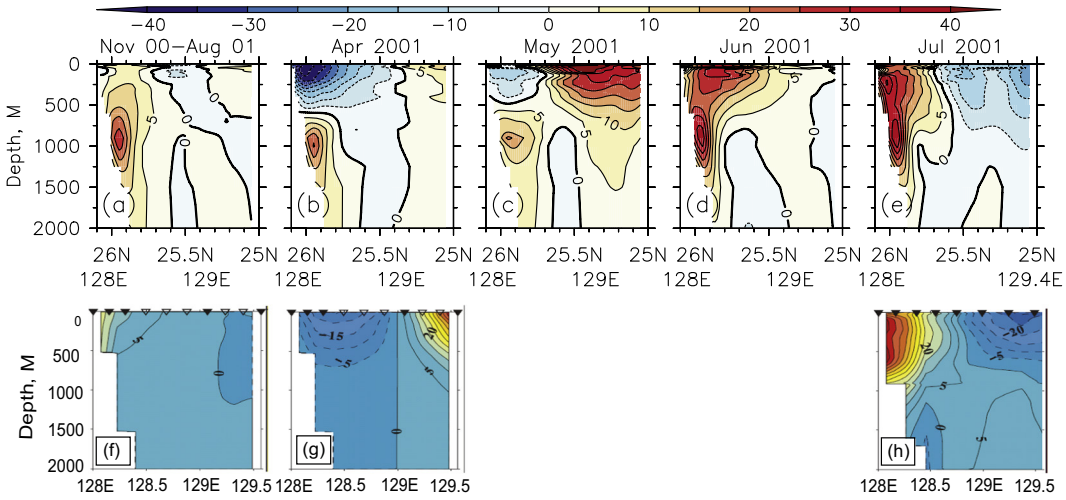


**Fig. 6.** Vertical sections of mean velocity (cm $s^{-1}$) from the reanalysis during (a) November 2000–August 2001, (b) April 2001, (c) May 2001, (d) June 2001, (e) July 2001 across the Okinawa section. Geostrophic velocity derived from the observations by Zhu et al. (2003, their Fig. 3) for the periods (f) November 2000–August 2001, (g) April 25, 2001 (cyclonic eddy), and (h) July 11–13, 2001 (anticyclonic eddy, absolute geostrophy) are included for comparisons. Note that the *x*-axis labels in (f–h) are different.

at ~1000 m depth. During the presence of the anticyclonic eddy (Fig. 6e), the northeastward current exhibits two velocity cores, one at ~200 m and the other at ~900 m, each with a velocity of 30 cm $s^{-1}$. As noted by Zhu et al. (2003), the current measured by the Acoustic Doppler Current Profiler (ADCP) set at 900 m on the slope was 25 cm $s^{-1}$ when anticyclonic eddy was present, so the geostrophic velocity relative to the sea bottom was not the best choice, as demonstrated in their Figs. 3c and 3d. It is worth noting that the reanalysis velocity at 900 m is 25 cm $s^{-1}$ and compares well with their absolute geostrophic velocity (their Fig. 3d).

The occurrence of two velocity cores in the reanalysis during the presence of the anticyclonic eddy has some resemblance to those in the observations (compare Fig. 6e and h). Similar current structures southeast of Okinawa are also reported by Yuan et al. (1994) during October–November 1991 with the first core located between 500 and 600 m (20 cm $s^{-1}$) and the other core seaward above 200 m. The observations by Liu and Yuan (2000) during February and April 1998 also showed a weak RCS core (700 m) below a strong cyclonic eddy, consistent with the reanalysis core in April 2001 (Fig. 6b). From the reanalysis, it is apparent that a weak, single core current structure during a cyclonic eddy is transformed into a strong, double core structure when an anticyclonic eddy occupies the region (Fig. 6b and e). The reanalysis velocity sections during May and June 2001 depicted in Fig. 6c and d provide a better description of this evolution. The remnants of a cyclonic eddy can still be seen in May 2001 on the shoreward side. A strong northeastward current (30 cm $s^{-1}$) on the offshore side is the manifestation of an approaching large anticyclonic eddy, as evident from the succeeding months. Its arrival in June 2001 leads to the intensification of the RCS, including the subsurface velocity core (~30 cm $s^{-1}$), owing to the flow acceleration driven by vertical shear. The eddy forms a distinct velocity core in the upper 200 m (~30 cm $s^{-1}$ at 25.8°N) on the seaward side of the deep RCS core. By July 2001, the shallow velocity core associated with the eddy deepens slightly (250 m) and moves farther shoreward overlying the deep velocity core (Fig. 6e). It should be noted here that a clear deep velocity core in Fig. 6e does not exist in the observed velocity section (Fig. 6h). This discrepancy seems to come from the limited resolution of the observations and the geostrophic calculation of the vertical structure of the observation-based current. For example, comparisons of velocity sections from Zhu et al. (2003) between the geostrophy and absolute geostrophy (referred to the shipboard ADCP) show a double core structure only in the absolute geostrophy (see their Figs. 3c and 3d).

We now compare the temporal evolution of vertical structure of velocity vectors from a long-term moored upward-looking ADCP with the reanalysis for the period December 2002–August 2004. The ADCP was located on the bottom slope east of Okinawa at 128.2°E, 26.2°N at a water depth of about 1077 m. Fig. 7a displays the velocity vectors at three depths, 500 m, 700 m and 830 m, from the ADCP (black) and reanalysis (red) along with the record mean vertical profiles of zonal (*u*, solid) and meridional (*v*, dashed) velocity components in Fig. 7b. The reanalysis adequately reproduces the current variability, but tends to underestimate the magnitude of velocity at 500 m and 700 m and overestimates it at 830 m. The current is predominantly northeastward at all depths with brief occasional southwestward currents associated with the passage of mesoscale eddies. The current is much more variable than that southeast of Amami-Ohshima. Both the reanalysis and observations show prolonged periods of weak currents during January–April 2003 and April–July 2004 (Fig. 7a). The horizontal structure of the circulation at 700 m near the RCS core in June 2004 (Fig. 7c) indicated a large anticyclonic eddy east of Kerama Gap (south of Okinawa), which caused a significant shift in the RCS path. As a result, neither a strong northeastward current nor a subsurface velocity core exist. The mean reanalysis velocity over the observation period shows a northeastward current below ~400 m and a subsurface velocity core between 800 m and 1000 m (Fig. 7b). This is consistent with the observations except that the ADCP maximum velocity occurs at 755 m with rapidly diminishing velocity below that. We should be cautious about the differences, because the model's closest grid point is deeper than the observation point.

A consistent pattern emerging from the reanalysis is the existence of a mean northeastward current with a subsurface velocity maximum between 800 m and 1000 m. A stronger (weaker) subsurface velocity core is accompanied by an approaching anticyclonic (cyclonic) eddy from east of Okinawa. In addition to the subsurface velocity core, a transient shallow velocity core appears at about 300 m followed by the anticyclonic eddies. On the other hand, the existence of an anticyclonic eddy just south of Okinawa (east of Kerama Gap) imposes a major shift in the RCS with no subsurface velocity maximum.

### 3.1.3. Miyakojima

Unlike other regions, the existence of both a stable northeastward current southeast of Miyakojima and a subsurface current core has not been explored due to limited observations. For the first time, we provide the temporal variations of the current

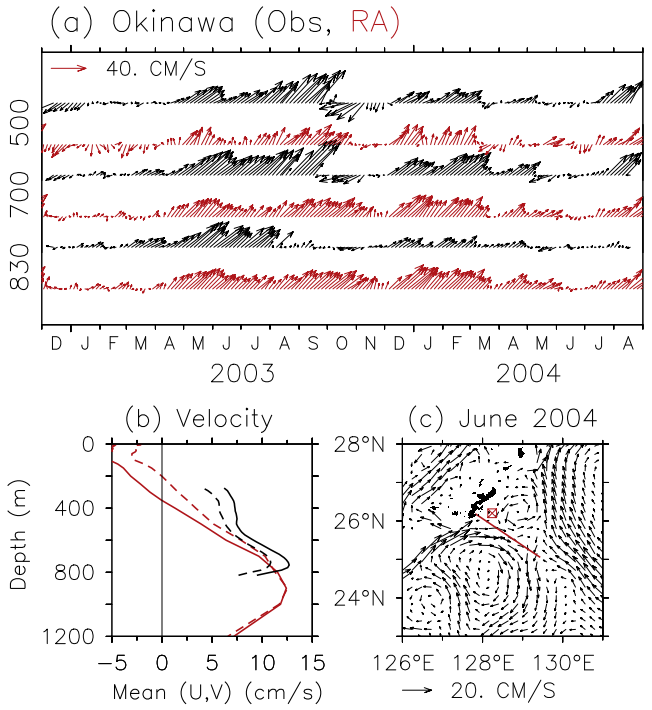


**Fig. 7.** Comparisons of (a) velocity vectors (cm $s^{-1}$) from the reanalysis (red) and moored upward-looking ADCP (Acoustic Doppler Current Profiler) observations (black) on the bottom slope southeast of Okinawa Island (128.2°E, 26.2°N) at 500 m, 700 m and 830 m during December 2002–August 2004, (b) temporal mean velocity components $u$ (solid) and $v$ (dashed) from the reanalysis (red) and ADCP (black), and (c) mean current at 700 m during June 2004 showing an anticyclonic eddy southeast of Okinawa; the red box marks the ADCP location. Velocity vectors have been smoothed using a 5-day moving average.

southeast of Miyakojima using current meter observations at two depths (570 m and 1240 m) and two nearby locations (126.04°E, 24.6°N, 126.05°E, 24.1°N) during December 2002–August 2004 (Fig. 8). Although the current meters are located slightly northeast of the Miyakojima section discussed here, their locations fall along the path of the RCS (Fig. 8, right panels). The current at 570 m in both the reanalysis (red vectors) and the observations (black vectors) is predominantly northeastward with large temporal variability. Again, the mesoscale eddies are responsible for the large variability, especially given the proximity of Miyakojima to the eddy-dominated region southeast of the Taiwan. Fluctuations in the currents reaching 20–30 cm $s^{-1}$ are accompanied by the passage of eddies. Compared to 570 m, the currents at 1240 m (water depth ~1600 m) do not show a predominant direction during the same period. Note that this location is sheltered from the RCS due to an ocean ridge, which is apparent in the spatial map of mean velocity at 1240 m. The mean currents during December 2002–August 2004 show a northeastward RCS at both depths (Fig. 8, right panels).

Do mesoscale eddies affect the vertical structure of the RCS southeast of Miyakojima? To explore this, we show examples of the RCS during the period of a cyclonic eddy and an anticyclonic eddy in Fig. 9. The current meter observations indicated a cyclonic eddy crossing the mooring site during March–April 2004 (Fig. 8). The vertical sections of velocity from the reanalysis during this period confirm a cyclonic eddy in the upper 500 m (Fig. 9a and b). There is a weak northeastward velocity core of 5–10 cm $s^{-1}$ below 500 m. As the overlying cyclonic eddy strengthens (>30 cm $s^{-1}$) the core velocity further weakens due to the vertical shear (Fig. 9b). The arrival of an anticyclonic eddy from the east in November 2004 leads to the collapse of the deep velocity core by merging with the northeastward current of the eddy (Fig. 9c). However, the eddy generates a shallow velocity core of 30 cm $s^{-1}$ at ~300 m. As the eddy weakens or drifts away, the deep core reappears at around 1000 m in depth, as seen in January 2005. It is clear that the impact of mesoscale eddies on the RCS structure southeast of Miyakojima is very similar to that southeast of Okinawa.

### 3.2. RCS structure and variability

#### 3.2.1. Mesoscale variability

It is evident from the preceding discussions that the significant variability of the current east of the Ryukyu Islands is dominated by mesoscale eddies. The 20-year reanalysis SSH and kinetic energy at 15 m provide a good measure of mesoscale variability. Fig. 10 depicts the SSH variability (standard deviation of the SSH in cm) and the eddy kinetic energy (EKE) and kinetic energy of the mean flow (KEM) from the reanalysis is shown in Fig. 11. A moderately large SSH variability (10–14 cm) and high EKE (600–700 $cm^2$ $s^{-2}$) on the eastern slope of Ryukyu Islands (offshore of Miyakojima and Amami-Ohshima) suggest that the mesoscale eddies from the interior ocean aid in the RCS variability. There is also a region of relatively strong SSH variability (14 cm) between Miyakojima and Okinawa in Fig. 10, which may be associated with the pathways of eddies entering the ECS through Kerama Gap, as evidenced by the intrusion of the 10 cm contour into the ECS. Northeast of Amami-Ohshima, the largest SSH variability (>16 cm) and high EKE (>700 $cm^2$ $s^{-2}$) occur along the Kuroshio northeast of Tokara Strait, encompassing the regions southeast of Kyushu and south of Shikoku (see Fig. 1 for location). The meandering of the Kuroshio south of Japan largely determines the location of the recirculation gyre. Since the RCS northeast of Okinawa is partially driven by the recirculation gyre (Fig. 12a and b), a region of large variability extending southwestward from the recirculation gyre has a direct impact on the RCS. High levels of EKE (>800 $cm^2$ $s^{-2}$) and SSH variability (~16 cm) in the region southeast of Taiwan are due to the arrival of westward propagating eddies generated by the shear between North Equatorial Current (NEC) and Subtropical Counter Current (STCC). When these mesoscale eddies merge with the Kuroshio, they generate offshore meandering and flow separation from the coast (Johns et al., 2001; Zhang et al., 2001) with a branch flowing east of the Ryukyu Islands, thereby contributing to the RCS variability. Unlike the Kuroshio, the KEM associated with the RCS is significantly weaker and only apparent for the RCS northeast of Okinawa. There is also a region of reduced KEM (<100 $cm^2$ $s^{-2}$) extending southwestward from the recirculation gyre, which joins the RCS northeast of Okinawa.

Adequately representing mesoscale eddies and the energy and enstrophy (dominated by smaller scales) cascades in ocean models is important in simulating the mean circulation. The comparisons of surface (15 m) EKE and KEM between the reanalysis and drifter observations clearly indicate that the reanalysis realistically reproduces the ocean energetics east of the Ryukyu Islands (Fig. 11). The drifter observations used here are discussed in Thoppil et al. (2011). Although similar patterns of EKE are seen in the reanalysis and the drifter observations east of the Ryukyu Islands, regions of high EKE in the reanalysis are closer to the Ryukyu Islands than that in the observations. This is an indication that the drifter observations do not account for all the mesoscale variability due to insufficient resolution and sampling frequency. As discussed in recent articles (e.g. Thoppil et al., 2011; Hurlburt et al., 2011 and references therein), the data assimilation has a major impact on the upper-ocean dynamics, especially in the vicinity of western boundary currents. The assimilation of ocean surface observations (especially eddies and current meanders) increases the mean flow

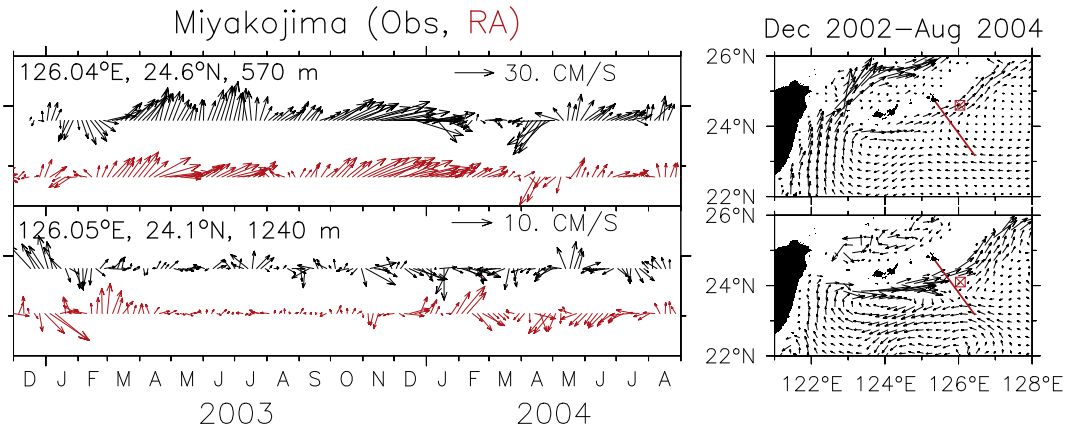


**Fig. 8.** Comparisons of velocity vectors (cm $s^{-1}$) from the reanalysis (red) and moored current meter observations (black) east of Miyakojima at two depths; 126.04°E, 24.6°N, 570 m (top left) and 126.05°E, 24.1°N, 1240 m (bottom left) during the period December 2002–August 2004. The mean currents at 570 m and 1240 m from the reanalysis during the observation period are shown to the right with the locations of the current meter observations. Velocity vectors have been smoothed using a 5-day moving average.

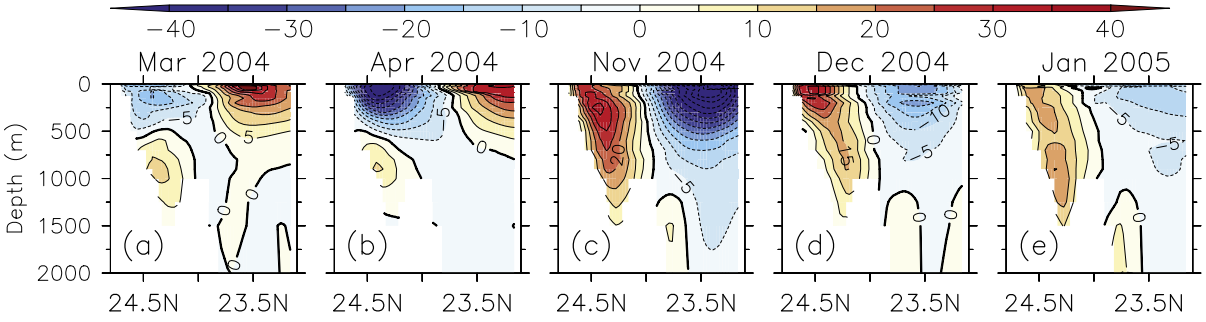


**Fig. 9.** Vertical sections of monthly mean velocity (cm $s^{-1}$) along Miyakojima during the presence of a cyclonic eddy (a) March 2004, (b) April 2004 and an anticyclonic eddy (c) November 2004 (d) December 2004, and (e) January 2005. The contour interval is 5 cm $s^{-1}$. Solid (dashed) contours indicate northeast (southwest) current. Note the impact of eddies on the RCS subsurface velocity core.

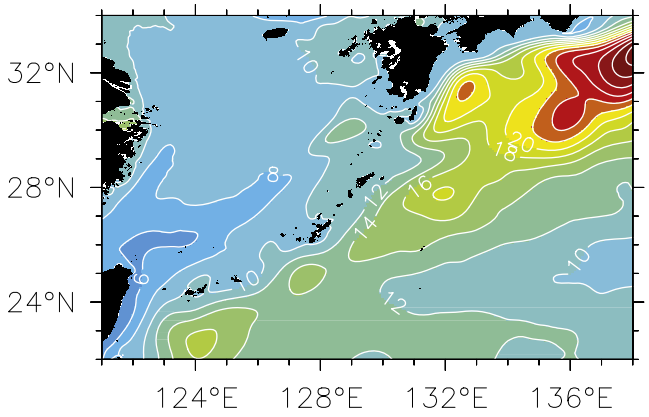


**Fig. 10.** Standard deviation of sea surface height (SSH in cm) from the reanalysis during 1993–2012. Contour interval = 2 cm. Regions of large mesoscale variability are evident east of the Ryukyu Islands.

of the entire water column by vertically transferring energy from the upper-ocean into the abyssal ocean. From a global comparison of EKE in a data-assimilative model with 712 moored current meter records, Thoppil et al. (2011) indicated an improved representation of the abyssal EKE.

*3.2.2. Mean RCS structure*

*3.2.2.1. Circulation in the upper 1500 m.* Unlike the Kuroshio in the ECS, a systematic study of the continuity of the RCS east of the Ryukyu Islands has yet to be made. Having validated the velocity structure at three locations against a variety of observations in Section 3.1, we now explore the continuity of the RCS using 20-years of reanalysis output. The horizontal structure of the RCS at 15 m in the reanalysis is compared with the observations of mean drifter velocity vectors (1990–2012) (Fig. 12a and b) at 15 m derived from the World Ocean Circulation Experiment (WOCE) Surface Velocity Program (SVP). The reanalysis reproduced major circulation features, including the Kuroshio in the ECS and its northward path after exiting the ECS through the Tokara Strait, the recirculation gyre, and the circulation east of the Ryukyu Islands, consistent with drifter observations. A well-developed northeastward-flowing RCS northeast of Okinawa is evident both in the reanalysis and observations and agrees with the mean field of surface velocity vectors presented in Fig. 3 of Nakamura et al. (2007). This current is partially fed by the southwestward extension of the anticyclonic recirculation gyre from the north with its southern flank penetrating farther south of Okinawa in the drifter observations than in the reanalysis. The center of the recirculation gyre in the reanalysis is located about 130 km southwest of that in the surface drifter observations (marked by triangles). This discrepancy may stem from the fact that the observations did not fully capture the various modes of the Kuroshio pathway south of Shikoku. The northeastward RCS between Miyakojima and Okinawa in the reanalysis appears to be part of an anticyclonic mesoscale circulation with a branch continuing north and merging with the returning branch of the recirculation gyre. Although both the reanalysis and observations show this feature, its center in the reanalysis is located farther north than the drifter observations (marked by diamonds).

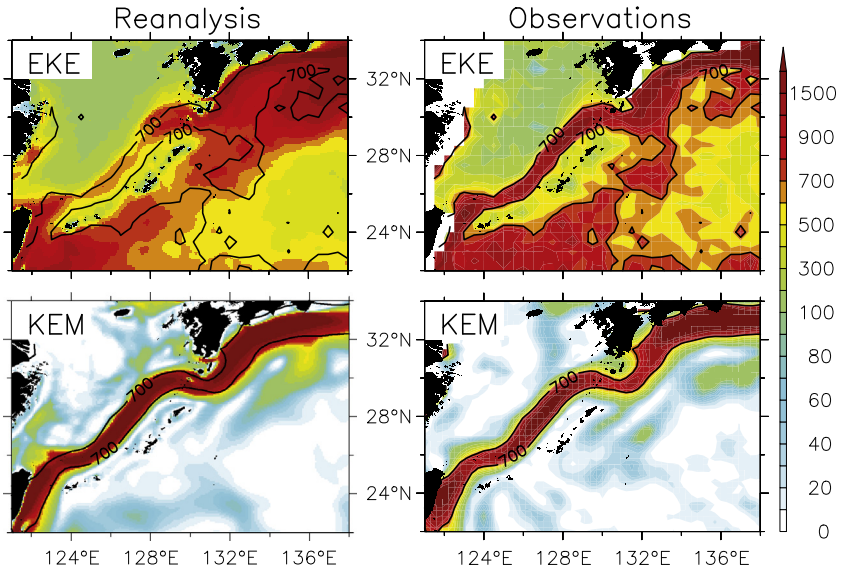


**Fig. 11.** (top) Surface eddy kinetic energy (EKE, $cm^2\ s^{-2}$) and (bottom) kinetic energy of the mean flow (KEM, $cm^2\ s^{-2}$) from the reanalysis (1993–2012) (left) and drifter observations (right) (see Thoppil et al., 2011 for details). For comparison, the 700 $cm^2\ s^{-2}$ contour from the observed EKE and KEM are superimposed on the reanalysis plots.

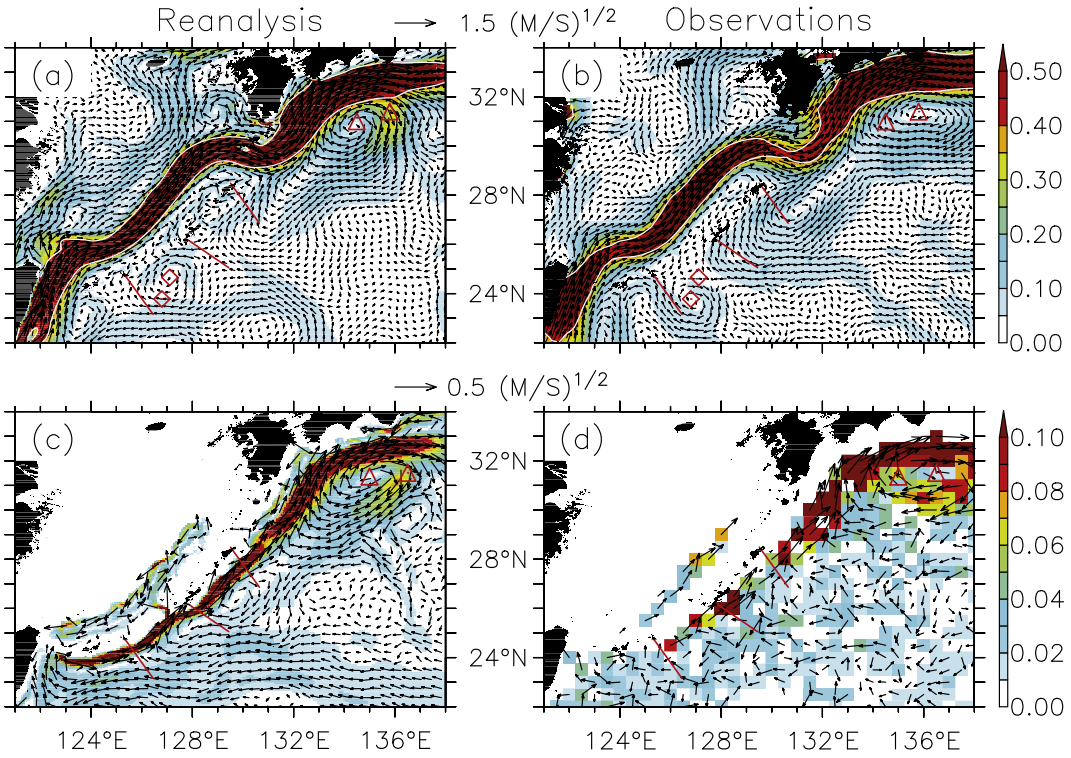


**Fig. 12.** Annual mean currents at 15 m (top) from (a) the reanalysis during 1993–2012 and (b) drifter observations during 1990–2012 and at 1000 m (bottom) from (c) the reanalysis and (d) Argo float observations with current speed shaded. For comparison, the 40 cm $s^{-1}$ contours are shown at 15 m. The 6-hourly drifter velocity vectors are interpolated to a 0.3°×0.3° grid using a Gaussian weighting function. The centers of the anticyclonic recirculation gyre from the reanalysis and the observations are marked with triangles along with the location of an anticyclonic eddy by diamonds. For clarity, each vector magnitude is divided by the square root of the speed.

The horizontal structure of the RCS at 1000 m in the reanalysis is compared with the observations of currents estimated from the Argo floats deployed prior to 2010 using the methods discussed in Ollitrault and Rannou (2013). It should be noted that the RCS lies below the sill depth of 700 m east of Taiwan. The RCS at 1000 m is different from that at 15 m with a notable difference in the circulation southwest of Okinawa (Fig. 12c and a). The reanalysis shows a well-developed continuous northeastward flowing RCS from east of Taiwan to northeast of Amami-Ohshima (Fig. 12c). The mean current is narrower than at the surface and reaches speeds exceeding 10 cm $s^{-1}$. The contribution from the recirculation to the RCS extends farther southwest to the southeast of Miyakojima whereas it is limited to the northeast of Okinawa at 15 m. The reanalysis also shows a weak westward current between 22°N and 24°N (2–4 cm $s^{-1}$), which merges with the RCS west of 128°E. The current structure in the reanalysis is in reasonable agreement with that derived from the Argo floats with three exceptions. In the observations, (1) a well-developed continuous RCS is evident only in the region northeast of Miyakojima (2) there is no clear shoreward RCS intensification and (3) no indication for a

southwestward extension of the recirculation gyre. These occurs because the number of Argo observations is inadequate to resolve such features. It is worth noting that the center of the recirculation gyre in the two independent surface drifter (Fig. 12b) and Argo observations (Fig. 12d) is the same.

The continuity of the RCS is further investigated at 200, 500, 700 and 1500 m depths (Fig. 13). The northeastward RCS emerges from northeast of Miyakojima at 200 m with its southwestward expansion to the east of Taiwan increasing in depth. As at the surface, the RCS between Miyakojima and Okinawa is influenced by an anticyclonic feature at 200 m. A weak RCS (<10 cm $s^{-1}$) first appears southwest of Miyakojima at 500 m and strengthens (>10 cm $s^{-1}$) at 700 m to form a continuous RCS from east of Taiwan to northeast of Amami-Ohshima. A stronger and wider RCS southeast of Amami-Ohshima than to the southwest (except at 1500 m) can be attributed to the contribution from the anticyclonic recirculation gyre. East of Taiwan between 123°E and 127°E, the RCS is connected to a westward current between 22°N and 24°N from 200 m to 1500 m, which becomes narrower with increasing depths. The Kuroshio bifurcation east of Taiwan appears to contribute very little to the origination of the RCS. The mean current at 1500 m is ~5 cm $s^{-1}$ along the RCS path. East of Amami-Ohshima (~28°N), part of the RCS veers offshore to form a large recirculation feature that rejoins the RCS northeast of Miyakojima. This offshore branch appears to block the contribution from the recirculation gyre.

*3.2.2.2. Abyssal circulation.* The deep current meter observations southeast of Amami-Ohshima indicated a northeastward current during January–May 2001 and a southwestward current during June–October 2001 at 1959 m (Fig. 4b, S6). The evolution of this flow reversal, which is manifested in the climatological monthly mean (1993–2012) currents at 2000 m, is illustrated in Fig. 14. Note that this flow reversal is not reflected at depths shallower than 2000 m (Fig. 13d) and the circulation becomes predominantly southwestward at depths deeper than 3000 m, consistent with the observations (Fig. 4b and c). There is a strong northeastward current (>5 cm $s^{-1}$) in January which in turn merges with the Kuroshio to form a continuous current downstream Amami-Ohshima. Part of the current southeast of Amami-Ohshima turns offshore with a branch returning southwestward. The current becomes much weaker in May and terminates southeast of Amami-Ohshima by turning offshore. The current southwest of Amami-Ohshima vanishes in July and is replaced by a southwestward current everywhere south of ~30°N by October. The southwestward current southwest of Amami-Ohshima vanishes by November (resembles July) and is replaced by a northeastward current in December (resembles January) (latter two figures not shown).

The emergence of a southwestward current south of 30°N can be ascribed to the combined effects of a cyclonic eddy and the recirculation gyre. Southeast of Kyushu and east of Tokara Strait, a shear-driven cyclonic eddy is seen at 1000 m depth on the inshore side of the Kuroshio (see inset, enclosed by a red box). The alongshore extent is determined by a deepening of the topography at either end (Fig. 1). At 2000 m, this eddy lies above the southern trench on the shoreward side of the overlying Kuroshio. A locally intensified cyclonic eddy in July appears to be the origin of southwestward current on the shoreward side. However, this cyclonic eddy may not be the only source triggering the southwestward current south of 30°N. Southeast of Kyushu, part of the recirculation gyre flows northwestward (enclosed by a dashed red box) on the southwest side of an ocean ridge (see Fig. 1). This current joins the seaward side of the overlying Kuroshio in both January and May and flows northeastward. By July, a major portion of the recirculation component feeds into the shoreward side of the cyclonic eddy and continues until October. The combined effect is the local intensification and southwestward expansion of the southwestward current down to Miyakojima. Thus our analysis suggests that the RCS at 2000 m between the east of Taiwan and Amami-Ohshima is northeastward from December to June and southwestward from August to October with July and November being the transition months.

### 3.3. Subsurface velocity core

#### 3.3.1. Annual mean

The mean velocity during the observation periods, discussed in Section 3.1, may have been aliased by mesoscale eddies. The 20-year reanalysis will provide an un-aliased mean velocity structure. As shown before, limited observations southeast of Amami-Ohshima and Okinawa indicated subsurface velocity cores (Ichikawa et al., 2004; Zhu et al., 2005), while the existence of a current core southeast of Miyakojima has not been reported previously. The vertical structure of the velocity across the three sections southeast of Miyakojima, Okinawa, and Amami-Ohshima, shown in Fig. 15a–c, reveals two important features: a mean northeastward current (positive velocity) and a well-developed current core at intermediate depths of 700–900 m. The current core east of Miyakojima is 12 cm $s^{-1}$ at 900 m and a weak southwestward current (−2 cm $s^{-1}$) in the upper 750 m on the offshore side (south of ~24°N) is associated with the westward current at 22°–24°N seen in Fig. 13. In the section southeast of Okinawa, the core velocity is 18 cm $s^{-1}$ with RCS confined to the north of 25.5°N. The modeling study of Nakamura et al. (2007) also indicated a current core in their section south of Okinawa, although the core was weaker than 10 cm $s^{-1}$ and deeper than 1000 m. The RCS southeast of Amami-Ohshima is wider than the other sections with a core velocity of 16 cm $s^{-1}$ at 700 m and resembles those presented in Fig. 2e. A southward expansion of the RCS south of 27.6°N in the upper 750 m on the offshore side is due to the contribution from the recirculation gyre joining the RCS. The northeastward current reduces to 8 cm $s^{-1}$ at 27.5°N near the surface. It should be noted that the magnitude of the current core is also sensitive to the choice of locations along the RCS path. The northeastward current in the lower layer is consistent with the upward tilting of isopycnal lines to the north at the depths below ~750 m. The velocity core lies on the 27.2 kg $m^{-3}$ isopycnal surface at Miyakojima and Okinawa and the 27 kg $m^{-3}$ at Amami-Ohshima. The standard deviation of the velocity shows peak variability in the upper few hundred meters with a secondary maximum coinciding with the current core (Fig. 15d–f).

#### 3.3.2. Interannual variability

The reanalysis successfully reproduced the large year-to-year variations of the subsurface velocity core observed southeast of Amami-Ohshima during December 1998–July 2002 (Fig. 2), which we have attributed to the mesoscale eddies (Fig. 3). To further explore the interannual variability during the 20-year reanalysis at three locations, we show the velocity anomalies (after removing the 1993–2012 mean) at the core depth of 750 m in Fig. 16 (shaded). The velocity anomalies have been smoothed using a 13-month Parzen filter to highlight the periods of strong and weak velocity cores at interannual time-scales. The core velocity southeast of Amami-Ohshima shows significant interannual variability with anomalies exceeding ±10 cm $s^{-1}$. The velocity core is weaker in 1995–96, 2008, 2012, 2006 and 2000 and a stronger core is evident in 1998, 1999 and 2011. Note that the core anomalies are weak during the period of the current meter observations, December 1998–July 2002. The anomalous core velocity southeast of Amami-Ohshima in 1995–96 can also be traced back to a much weaker core southeast of Okinawa at an earlier time in 1994–95. The periods of strong (weak) current core coincide with positive (negative) SSHA, shown as red lines in Fig. 16. The pattern of SSHA

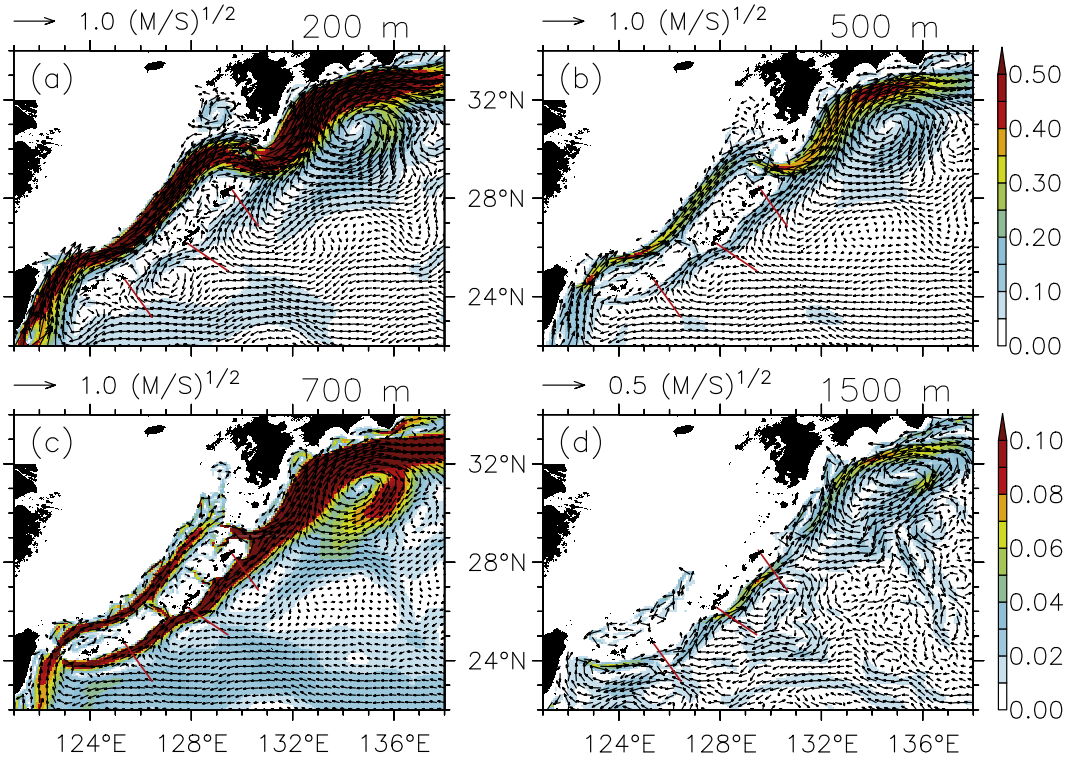


**Fig. 13.** Annual mean currents at (a) 200 m, (b) 500 m, (c) 700 m and (d) 1500 m from the reanalysis during 1993–2012 with current speed (m $s^{-1}$) shaded. For clarity, each vector magnitude is divided by the square root of the speed. Note that different reference vectors are used.

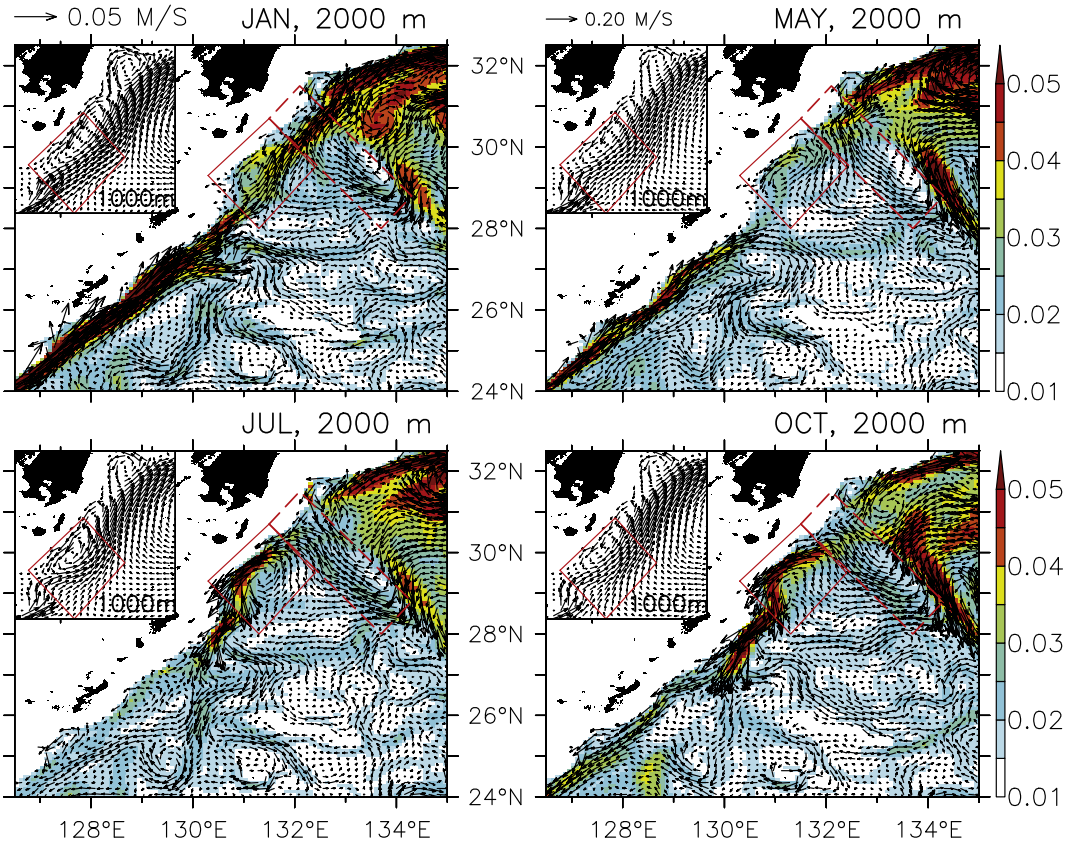


**Fig. 14.** Monthly mean climatology (1993–2012) of currents at 2000 m for January, May, July and October with the current speed shaded in m $s^{-1}$. The inset plot shows the mean current at 1000 m zoomed into the region south of Kyushu Island for the same months. The reference vector is 0.05 (0.2) m $s^{-1}$ at 2000 m (1000 m). The current east of Ryukyu Islands shows a seasonal reversal at 2000 m. The solid box indicates the location of a cyclonic circulation and a dashed box marks its contribution from the recirculation gyre.

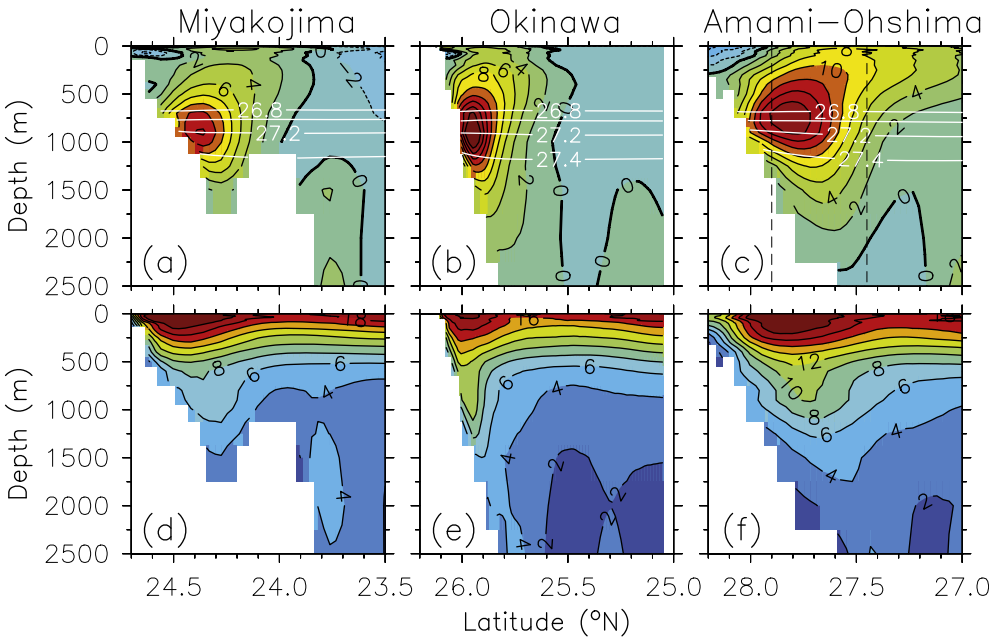


**Fig. 15.** Vertical sections of (top) mean velocity (cm $s^{-1}$, black contours) and density between 26.8 and 27.4 kg $m^{-3}$ (white contours) and (bottom) standard deviation of velocity (cm $s^{-1}$) southeast of Miyakojima, Okinawa and Amami-Ohshima from the reanalysis during 1993–2012. The dashed lines in (c) indicate the region bounded by the current meter observations of Ichikawa et al. (2004). The existence of a subsurface velocity maximum in all the sections is a prominent feature. The location of these sections is shown in Fig. 1.

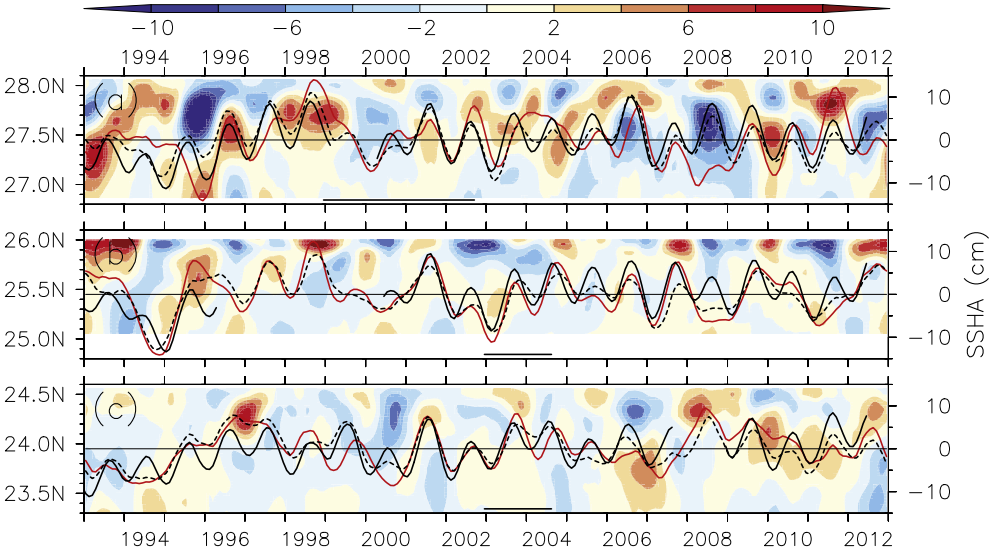


**Fig. 16.** Reanalysis velocity anomalies (cm $s^{-1}$, shaded) at 750 m depth obtained after removing the annual mean 1993–2012 across the sections southeast of (a) Amami-Ohshima, (b) Okinawa and (c) Miyakojima. They depict the interannual variation of current core velocity associated with the RCS. Area averaged sea surface height anomalies (SSHA, cm) for the regions (a) Amami-Ohshima (129.5°–131.5°E, 27°–28.5°N), (b) Okinawa (127.5°–129.5°E, 25°–26.5°N) and (c) Miyakojima (125°–127°E, 23.5°–25°N) are plotted as a red line. Also included are comparisons of coastal tide-gauge SSHA observations (solid black line) at 129.5°E, 28.5°N (Amami-Ohshima), 127.82°E, 26.18°N (Okinawa), and 124.16°E, 24.33°N (Miyakojima) with the reanalysis (dashed black line). To highlight the interannual variability, a 13-month Parzen filter is applied to these time-series. Horizontal lines highlight the current meter observations period discussed in the text.

is consistent with the sea level anomalies obtained from the tide gauges at the coastal stations of Amami-Ohshima (129.5°E, 28.5°N), Okinawa (127.82°E, 26.18°N), and Miyakojima (124.16°E, 24.33°N), as shown by black lines in Fig. 16. The corresponding values from the reanalysis are shown as dashed lines. The correlation coefficients between tide gauges (black lines) and the reanalysis (dashed lines) SSHA at three locations are 0.88, 0.68 and 0.83 respectively and their correspondence with the velocity anomalies at 750 m provide some confidence in the reanalysis interannual variability. The large discrepancy between the area averaged SSHA (red) and the tide-gauge SSHA (solid and dashed black lines), seen for example in 2008, stems from the fact that these point observations are indicative of the sea level at the coast (northernmost part of the sections).

In the following, the relationship between the core velocity and the offshore circulation pattern is examined with a focus on the Amami-Ohshima region. Using periods of strong (1998, 1999, 2011) and weak (1995, 2006, 2008, 2012) velocity cores, composite maps of vector velocity anomalies at 750 m depth are shown in Fig. 17a and b and overlaid on the SSHA (shaded). It is clear that

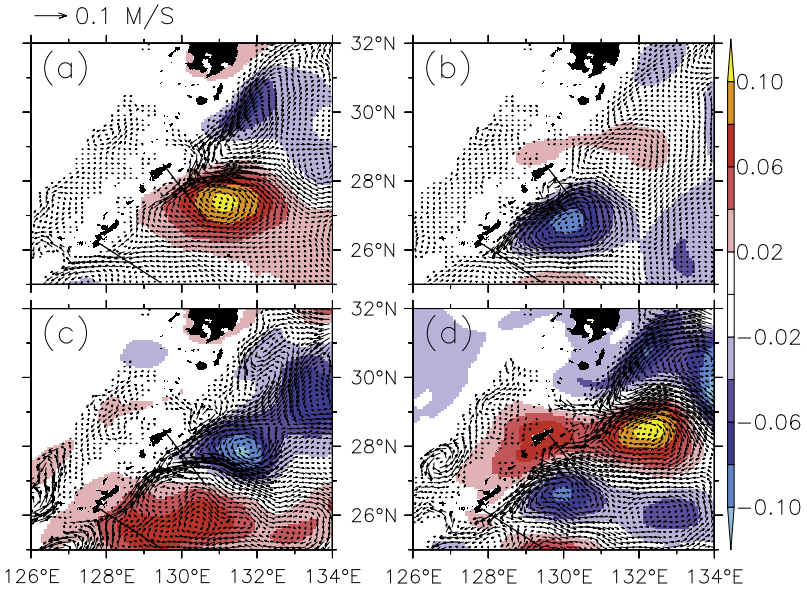


**Fig. 17.** Mean circulation anomalies relative to 1993–2012 at 750 m (vectors) and SSHA (m, shaded) based on the periods of (a) strong (1998, 1999, 2011), (b) weak (1995, 2006, 2008, 2012) RCS velocity cores, and (c) July 2009–July 2010 and (d) January 2006–December 2006 southeast of Amami-Ohshima. An anticyclonic (cyclonic) circulation exists during the periods of strong (weak) RCS cores (a and b) and two alongside eddies with opposite circulation are evident in (c and d).

a stronger current core southeast of Amami-Ohshima is accompanied by an anticyclonic circulation and a weaker core by a cyclonic circulation, corresponding to a high and a low in the SSHA. There is also an anomalous southwestward current downstream of Amami-Ohshima, which appears to be part of a large cyclonic circulation. It merges into the northeastward flow east of Amami-Ohshima, thereby weakening the current on the onshore side while strengthening on the offshore side (Fig. 17a).

There is an apparent discrepancy between the core anomaly and SSHA during 2009–2010 (2006), when the core anomaly is positive (negative) despite a low (high) in the SSHA (Fig. 16a). A possible explanation is the presence of two adjacent eddies of opposite sign. To clarify this point, we show SSHA (shaded) and velocity anomalies at 750 m for the periods July 2009–July 2010 and January–December 2006 in Fig. 17c and d, respectively. During both periods, mesoscale eddies of opposite sign meet southeast of Amami-Ohshima at about ~27°N. During the former period (Fig. 17c), a large anticyclonic eddy to the southeast and a cyclonic eddy to the east of Amami-Ohshima generate a northeastward (southwestward) current on the offshore (onshore) side of the section. The circulation becomes opposite during the latter period 2006, due to the changes in the polarity of the mesoscale eddies (Fig. 17d).

A close correspondence between the velocity anomalies at 750 m and SSHA in Fig. 17 suggest that the source of eddies and their propagation can be inferred from the SSHA. The Hovmöller diagrams of SSHA at 25°N (Miyakojima), 26°N (Okinawa) and 28°N (Amami-Ohshima), displayed in Fig. 18 after smoothed using a 15-month Parzen filter, show a banded structure with positive and negative anomalies. As expected, the periods of strong and weak velocity core coincide with the arrival of positive and negative SSHA from the east. These are the signatures of discrete eddies, which propagate westward roughly at the speed of non-dispersive, first internal mode Rossby waves. A negative SSHA slope, indicative of westward propagation, can be identified in some years. For example, at 25°N there is a negative SSHA starting around 2006 at 170°E and a positive event starting around 2002. The anomalies of the 18°C isotherm also show a similar banded structure with positive (negative) values, indicating deepening (shoaling) of the thermocline (not shown), that is highly correlated with the SSHA. The speed estimated from the slope of the negative SSHA during 2006–2008 is ~6.2 cm $s^{-1}$, which is close to the Rossby wave speed of ~6.7 cm $s^{-1}$ at ~25°N, with a similar speed obtained during 2002–2004 from a positive SSHA, and the inferred speed from a negative SSHA during 1993–94 is 6.6 cm $s^{-1}$. However, a positive SSHA during 1998–99 propagates with a speed of ~13.7 cm $s^{-1}$ with an eddy signature similar to one seen in 1993–94 (Amami-Ohshima). It is also apparent that some westward propagating eddies are generated or amplified by flow forced through the Izu-Ogasawara Ridge (west of ~145°E). In particular, its effect is very evident at 28°N. In a numerical model, Isobe and Imawaki (2002) investigated the role of the Izu Ridge on the westward propagation of Rossby waves and their impact on the Kuroshio transport. They found the Kuroshio transport variability associated with the Rossby waves is modified by the Izu Ridge.

### 3.4. Volume transport

#### 3.4.1. Annual cycle

The previously-estimated volume transports southeast of Amami-Ohshima and Okinawa vary widely due to limited observations that are aliased by mesoscale eddies and geostrophic calculations that assume a level of no motion. The volume transport across the three sections is calculated using the velocity component normal to the sections from a 20-year reanalysis (Fig. 19a). The volume transport southeast of Amami-Ohshima ranges between 6 Sv (August) and 18 Sv (December) with a mean value of 12.4 Sv, which is slightly lower than the observed mean of 16 Sv in the upper 1500 m over the 4.5-year period found by Ichikawa et al. (2004). The transport gradually decreases from January (16.6 Sv) to October (7.2 Sv) followed by a rapid increase from October to December. Except for the magnitude, transport southeast of Okinawa shows a similar seasonal pattern, minimum during July–October (2.4 Sv) and maximum during December–February (11 Sv). The mean transport is 6.2 Sv, which is larger than the 4.5 Sv obtained from the altimeter observations during 1992–2001 by Zhu et al. (2004). It should be noted that Zhu et al. (2004) employed an empirical relationship between a 270-day time-series of geostrophic volume transport and differences in sea surface height anomaly in order to obtain their long-term

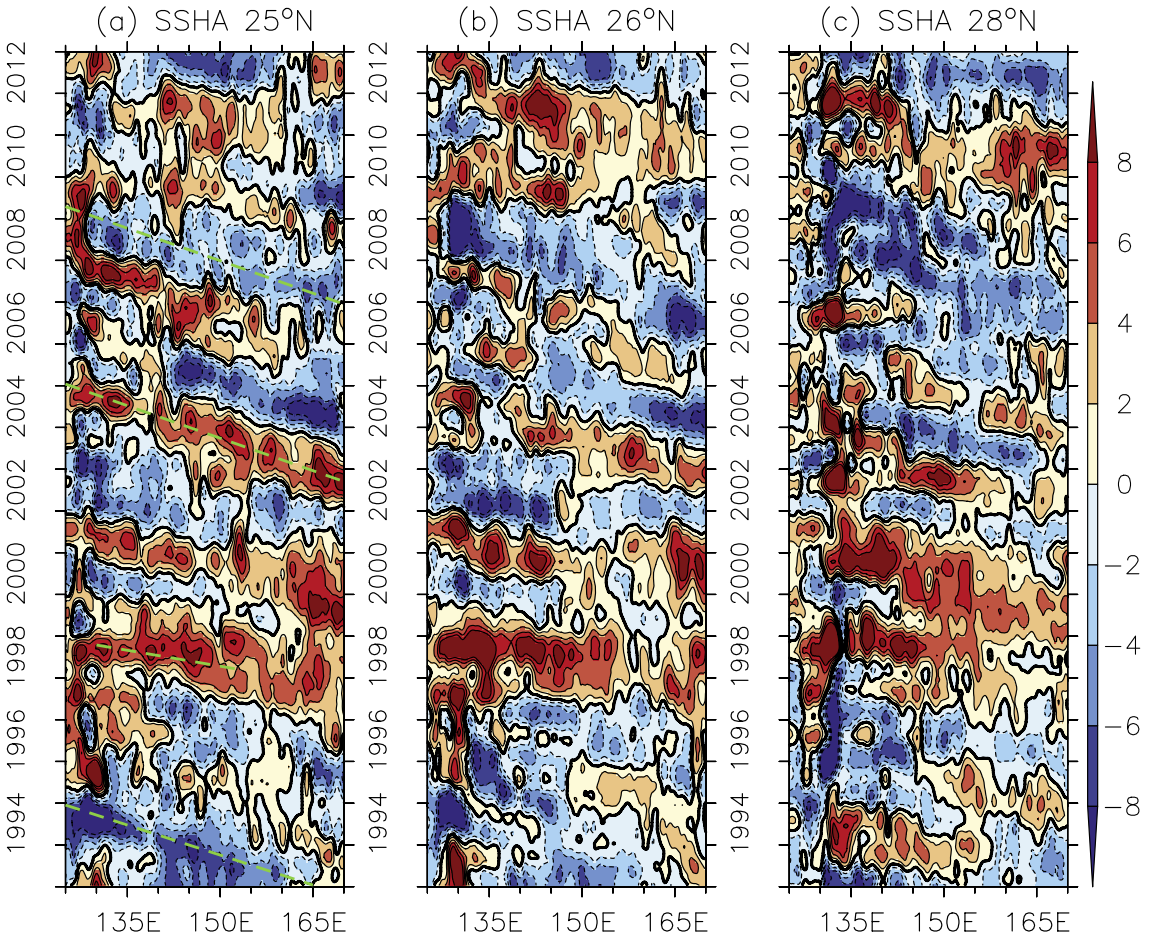


**Fig. 18.** Hovmöller diagram of SSHA (cm) at (a) 25°N, (b) 26°N, and (c) 28°N for the Miyakojima, Okinawa and Amami-Ohshima regions respectively. The dashed green lines indicate the westward propagating cyclonic and anticyclonic eddies. The average propagation speed estimated from the slope during the three periods (1993–94, 2002–04, and 2006–08) is 6.4 cm $s^{-1}$ at 25°N. A 15-month Parzen filter is applied to these time-series. Contour interval is 2 cm.

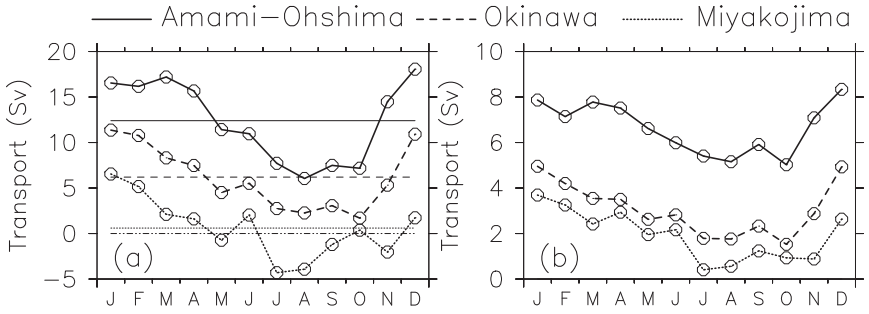


**Fig. 19.** Annual cycle of volume transport in Sv (1 Sv ≡ $10^6$ $m^3$ $s^{-1}$) across the sections southeast of Miyakojima, Okinawa, and Amami-Ohshima during the period 1993–2012 integrated (a) over the entire water column and (b) between 500 m and 1500 m. Annual mean values are indicated by thin lines. Positive (negative) values indicates northeastward (southwestward) transport. The annual cycle shows a winter maximum and a summer minimum.

transport. The transport ranges between −4.3 Sv (July) and 6.5 Sv (January) southeast of Miyakojima with a mean value of 0.6 Sv. The transport becomes southwestward from July to September and again in November. Note that the southwestward transport southeast of Miyakojima does not necessarily reflect a missing northeastward current, rather it is an indication that the Miyakojima section extends farther offshore and includes part of the westward current. It is evident from Figs. 12 and 13 that the offshore extent of the RCS increases from southeast of Miyakojima to Amami-Ohshima. By limiting the calculation to northwest of 23.7°N, the mean transport southeast of Miyakojima increases to 4.5 Sv. Conversely, the mean transport reduces to 5.0 Sv southeast of Okinawa when the calculation is performed northwest of 25.4°N. Since the offshore extent of the RCS across these sections is difficult to define, we believe that the transport values are representative of the RCS.

Since the depth of the subsurface velocity core lies well below the Ekman layer, the annual cycle of volume transport may represent the effect of the seasonal cycle of the velocity core. To examine this, we show the annual cycle of transport integrated between 500 m and 1500 m in Fig. 19b. The resulting transport shows an annual cycle that is similar to the total volume transport (Fig. 19a)

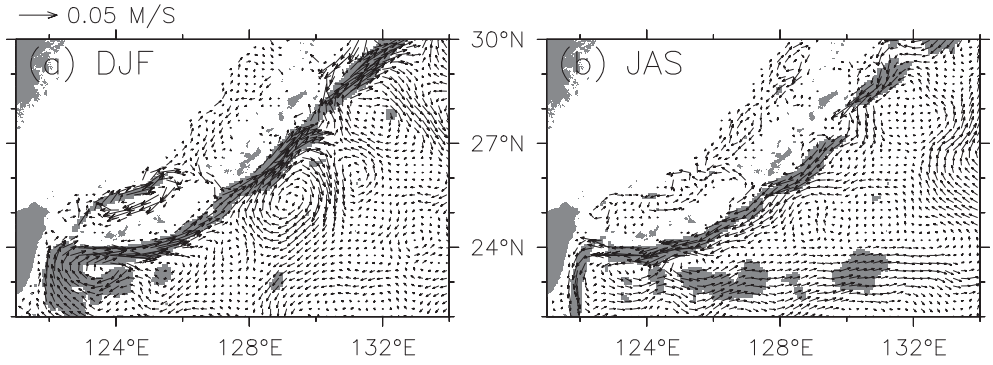


**Fig. 20.** Circulation anomalies (1993–2012 mean removed) at 750 m for (a) winter (December–February) and (b) summer (July–September). The speed anomalies (a) >0.01 m $s^{-1}$ and (b) <0.01 m $s^{-1}$ are shaded. These circulation patterns are consistent with the annual cycle of volume transport with maximum transport in winter and minimum in summer.

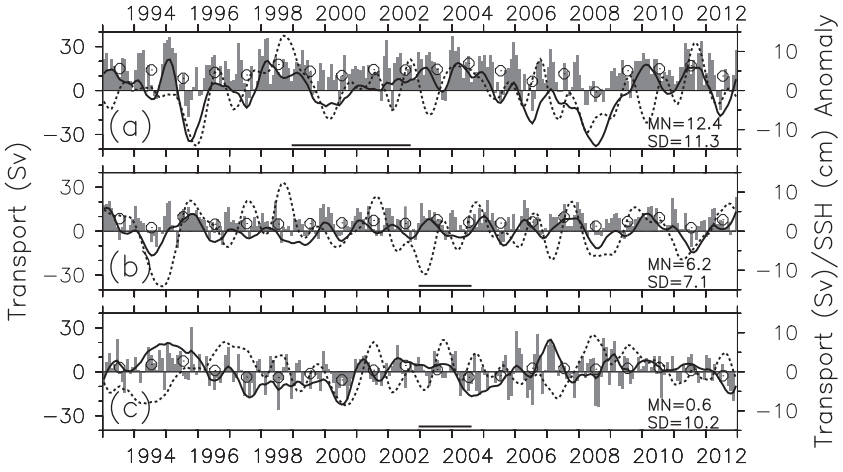


**Fig. 21.** Interannual variations of volume transport in Sv across the (a) Amami-Ohshima, (b) Okinawa, and (c) Miyakojima sections, shown as filled grey histograms. The 1993–2012 mean (MN) and standard deviations (SD) are denoted. Transport anomalies (solid line) and area averaged SSHA (dotted line, cm) after smoothing with a 13-month Parzen filter are shown in each panel together with yearly averaged transport values (circles). Area averaged SSHA are for (a) Amami-Ohshima (129.5°–131.5°E, 27°–28.5°N), (b) Okinawa (127.5°–129.5°E, 25°–26.5°N) and (c) Miyakojima (125°–127°E, 23.5°–25°N). The interannual standard deviation is 4.3 (Amami-Ohshima), 2.1 (Okinawa) and 3.3 Sv (Miyakojima). Horizontal lines highlight the current meter observations period discussed in the text.

with a maximum in winter and a minimum in summer. The mean transports of the subsurface core related component for the regions southeast of Amami-Ohshima, Okinawa and Miyakojima are 6.7 Sv, 3.1 Sv and 1.9 Sv respectively. The seasonal variation of the subsurface velocity core is depicted in Fig. 20, which shows the anomalies (1993–2012 mean) of velocities at 750 m for winter (December–February) and summer (July–September). An anomalous northeastward (southwestward) current in winter (summer) is consistent with the annual cycle of volume transport. These results suggest that subsurface velocity has a stronger (weaker) core in winter (summer) and that the annual cycle of transport is mainly due to the annual cycle of subsurface velocity core.

### 3.4.2. Interannual variability

Satellite derived SSHA has been used to provide long-term monitoring of the transport across major western boundary currents such as the Kuroshio south of Japan by Imawaki et al. (2001). However, the RCS is not identifiable from satellite altimetry because it is significantly weaker than the Kuroshio and it has a subsurface velocity maximum. Thus, the utility of altimetry is limited to certain regions, despite being used for the estimation of transport southeast of Okinawa by Zhu et al. (2004). The interannual variation of the volume transport from 1993 to 2012 across the three sections is shown in Fig. 21 (grey histograms) from the reanalysis. The transport southeast of Amami-Ohshima ranges from −18 (September 1995) to 37 Sv (January 2004) with a standard deviation of 11.3 Sv. The transport is northeastward during most of the period, but it is southwestward occasionally for short periods. The mean during the period of current meter observations (December 1998–July 2002) is 12.6 Sv (consistent with the 1993–2012 mean of 12.4 Sv), with a peak transport of 34.5 Sv in December 2001 associated with an anticyclonic eddy (Fig. 4a). The yearly-averaged transport (circles) shows a maximum in 2004 (18.6 Sv) and a minimum in 2008 (−1.1 Sv) with a standard deviation of 4.3 Sv. The interannual variability, which is shown as a transport anomaly obtained by subtracting the 1993–2012 mean, is plotted (solid line) after applying a 13-month Parzen smoothing. The resulting transport anomaly generally correlates well with the SSHA (dotted line) and the RCS core variability with anomalous southwestward transport occurring in 1995–96, 2006, 2008, and 2012, coinciding with the periods of weak subsurface velocity core (Fig. 16a). The northeastward transport peaks during 1994–95, 1998, 2004, 2009–2010, and 2011. As revealed by SSHA in Fig. 18, a large part of this variability can be ascribed to the arrival of mesoscale eddies from the east. For example, the arrival of an anticyclonic (cyclonic) eddy in 1998 (2008) resulted in a northeastward (southwestward) transport anomaly. However, an apparent discrepancy between the transport anomaly and SSHA is evident during 2009–2010 (2006)

when the transport anomalies are northeastward (southwestward), despite a low (high) in the SSHA. As shown in Fig. 17c and d, the presence of two adjacent eddies of opposite sign during these periods dominated the transport anomalies.

The variation of volume transport southeast of Okinawa ranges from −11 Sv (May 1995) to 23 Sv (December 2012) with a standard deviation of 7.1 Sv (Fig. 21b), which is slightly larger than the 5.5 Sv obtained by Zhu et al. (2004). The yearly mean transport is always northeastward (circles) with an interannual standard deviation of 2.1 Sv, which is only ∼50% of that southeast of Amami-Ohshima. The interannual variability is dominated by the seasonal patterns with transport anomalies (solid line) fluctuating between northeastward in winter and southwestward in summer months (±5 Sv). This is consistent with the seasonal anomalies of currents at 750 m, which shows a northeastward current in winter and a southwestward current in summer (Fig. 20). Modulation of winter transport variability by an anticyclonic eddy southeast of Okinawa is also evident (Fig. 20a). In addition to the seasonal dominance, the interannual variability is influenced by mesoscale eddies from the east. For example, the positive transport anomalies (and SSHA) in 2000–2001, 2004–2005, 2009–2010 and 2012 can be explained by the westward propagating anticyclonic eddies (Fig. 18b) and the arrival of a cyclonic eddy in 2008 generates a −4.4 Sv transport anomaly (and SSHA).

The volume transport southeast of Miyakojima fluctuates widely between northeast and southwest with values ranging from −25 Sv (July 1998) to 30 Sv (October 1995) with a standard deviation of 10.2 Sv around a mean northeastward transport of 0.6 Sv (Fig. 21c). Note that the variability is so large that on a comparative basis the mean transport is close to zero. For the variation at intra-seasonal time-scales, the rapid fluctuations can be associated with the mesoscale eddies arising from the sheared flow between the NEC and the STCC (18°–25°N). Current meter observations indicated a cyclonic eddy followed by an anticyclonic eddy in 2003–2004 (Fig. 8) and a corresponding change in the volume transport is evident in Fig. 21c. Another source of variability is associated with the offshore meandering of the Kuroshio east of Taiwan with a part of the Kuroshio taking a route southeast of the Ryukyu Islands (Johns et al., 2001; Zhang et al., 2001). Johns et al. (2001) reported a large meandering event in October 1995, which generated a maximum northeastward transport of 30 Sv during the 20 years, although the associated increase across the northern sections in the following months is less clear. Johns et al. (2001) also observed a significant reduction in the Kuroshio transport east of Taiwan during this period. However, its contribution to the interannual variability is negligibly small.

The transport anomaly undergoes a positive phase (northeastward) during 1994–1995 (7.4 Sv) and negative phases (southwestward) during 1997–2000 (−8.4 Sv) and 2004–2005 (−6.2 Sv). As discussed before, the transport anomalies can be explained, among other variables, by mesoscale eddies from the east and eddy-eddy interaction. The negative (positive) transport anomaly in 2000 (2001) can be ascribed to the arrival of a cyclonic (anticyclonic) eddy from the east (Fig. 18a). However, the southwestward (northeastward) transport anomaly in 2004–2005 (2002–2003) contrasts with an anticyclonic (cyclonic) eddy (Fig. 18a), which can be attributable to the presence of two adjacent eddies.

## 4. Summary and conclusions

The Ryukyu Islands form a boundary between two western boundary currents, the strong Kuroshio flowing through the East China Sea to the west and a weaker Ryukyu Current System (RCS) to the east, the latter being strongly affected by mesoscale eddies from the North Pacific. Previously, the structure of the RCS between east of Taiwan and east of Tokara Strait had only been determined using short-term current meter or snapshot hydrographic observations. Limited by their spatial and temporal scales, these observations indicated a northeastward current, though at times its presence was masked by eddy variability. Yet, until now the structure and variability of the RCS, based on a long-term analysis, has remained unexplored. Here, output from a 32-layer, 1/12.5° horizontal resolution global HYCOM/NCODA reanalysis for the period 1993–2012 (20 years) is used to study the mean structure of the RCS and its variation with particular attention to three locations southeast of Miyakojima, Okinawa, and Amami-Ohshima along the path of the RCS. This is achieved primarily by focusing on the existence of a subsurface velocity maximum associated with the RCS and its variability, followed by comparing the results from a variety of velocity observations with the reanalysis. The characteristics of the RCS depicted in the observations are well represented in the reanalysis. These include a predominantly northeastward current often interrupted by mesoscale eddies southeast of Amami-Ohshima at intermediate depths, flow reversal at depths deeper than 2000 m, a subsurface velocity core, and structure and variability resulting from the mesoscale eddies. These comparisons not only enhance confidence in our model simulation, but also add value to the observations by filling in the spatial as well as temporal gaps.

The horizontal structure of the mean RCS at 15 m shows a well-developed northeastward current northeast of Okinawa. This current is partly fed by the southwestward extension of the anticyclonic recirculation gyre from the north, whose contribution leads to a wider RCS northeast of Okinawa. The RCS southwest of Okinawa is disorganized and appears to be influenced by an anticyclonic circulation between Miyakojima and Okinawa, which has not been previously reported. Below 500 m, the RCS forms a continuous northeastward current from Miyakojima to Amami-Ohshima consistent with the Argo float observations at 1000 m. East of Taiwan, the RCS is fed by the westward currents at 22°–24°N. A part of the RCS veers offshore southeast of Amami-Ohshima due to bathymetry at 1500 m, which rejoins the RCS southeast of Miyakojima.

The most notable circulation feature is the seasonal flow reversal at 2000 m. The RCS between east of Taiwan and Amami-Ohshima is northeastward from December to June and southwestward from August to October with July and November being the transition months. The origin of this quasi-steady southwestward current from August to October can be traced to a cyclonic circulation southeast of Kyushu at 30°N (132°E). Southeast of Kyushu and east of Tokara Strait, a shear-driven cyclonic circulation forms at 1000 m on the inshore side of the Kuroshio. This lies above the southern trench at 2000 m on the shoreward side of the overlying Kuroshio. This forms a southwestward current south of 30°N with further intensification due to the contributions from the recirculation gyre. The circulation is predominantly southwestward at depths deeper than 3000 m. While bathymetric features are important in steering the deep currents especially in the downstream Amami-Ohshima region, the Kuroshio path southeast of Kyushu and east of Tokara Strait, the location of recirculation gyre, and the seasonal changes in the RCS volume transport are suggested to be the other key factors in the mechanisms underlying the RCS. On the basis of our model-observation comparisons and previous studies, a revised schematic of the circulation east of the Ryukyu Islands is inferred and shown in Fig. 1.

A distinct feature of the RCS is the existence of a subsurface velocity maximum at intermediate depths. The mean vertical structure of the RCS reveals a northeastward current and a subsurface velocity core at 700 m southeast of Amami-Ohshima and at 900 m southeast of Okinawa and Miyakojima with core velocities of $\sim$16 cm s$^{-1}$, $\sim$18 cm s$^{-1}$, and $\sim$12 cm s$^{-1}$, respectively. A modulation of the

vertical structure of the velocity core by the overlaying mesoscale eddies from the interior ocean is found across all three sections. An anticyclonic eddy often accompanies a two-core velocity structure, with the surface core confined in the upper 300 m and a deeper core at about 700–900 m. A cyclonic eddy is accompanied by a weaker deeper core. On the interannual time-scale, the mesoscale eddies generate anomalies of core velocities exceeding ±10 cm $s^{-1}$.

The volume transport (integrated over the entire water column) across the three sections show a clear annual cycle with a maximum transport during winter-spring and a minimum in summer. When the calculation is limited within the subsurface velocity core, excluding the Ekman contribution, the resulting transport also showed a clear annual cycle. This suggests that the annual cycle in the transport is primarily due to the annual variation of the strength of the velocity core, which shows an anomalous northeastward (southwestward) current in winter (summer). The annual mean shows a northeastward transport, which increases from 0.6 Sv (Miyakojima) to 6.2 Sv (Okinawa) to 12.4 Sv (Amami-Ohshima) with standard deviations of 10.2 Sv, 7.1 Sv, and 11.3 Sv, respectively. An increase of 6.2 Sv from Okinawa to Amami-Ohshima is due to the contribution from the southwestward extension of the recirculation gyre that joins the RCS northeast of Okinawa. The large transport variability southeast of Amami-Ohshima (11.3 Sv) can be in part ascribed to the fluctuations in the recirculation gyre. Part of the variability reflects the dominant role of mesoscale eddies in modulating the transport.

The monthly means of volume transport southeast of Amami-Ohshima during 1993–2012 range between −18 Sv (southwestward) and 37 Sv (northeastward) with an interannual standard deviation of 4.3 Sv. Transport anomalies >5 Sv (<−5 Sv), after removing 1993–2012 mean, coincide with the periods of strong (weak) velocity cores, which are correlated with the impinging mesoscale eddies from the interior ocean. The transport anomalies southeast of Okinawa are dominated by the seasonal variations with large (small) northeastward (southwestward) transport during winter (summer) months. The transport southeast of Miyakojima fluctuates rapidly between northeast and southwest on intra-seasonal scales due to the enhanced mesoscale eddies arising from the sheared current between the STCC and NEC. Besides eddies, extreme transports of ∼30 Sv within a month are associated with the meandering of the Kuroshio east of Taiwan. Similar patterns of variability in the volume transport, subsurface velocity core, and SSHA along the three sections during the 20-year reanalysis suggest that the mesoscale eddies are the source of significant interannual transport variability of the RCS in the regions from Miyakojima to Amami-Ohshima.

For the first time, we infer a detailed description of the circulation and its variability east of the Ryukyu Islands by using the 20 years of reanalysis output. The reanalysis not only helps fill in gaps in the observations, but it is also valuable in gaining insight into the physical mechanisms. While the structure and variability of the RCS is well represented in the reanalysis, the magnitude and depth of the current core differ from the observations. Our preliminary analysis links this model-data discrepancy to the synthetic profiles that are used in the data-assimilative system, but more work is needed to establish a causal relationship. A consistent result emerging from the analysis is the significant impact of eddies on the RCS structure and variability on time scales ranging from intra-seasonal to interannual. Long-term ocean current measurements are needed to confirm the inferred annual cycle of the volume transport that may be modulated by the seasonal variation of the impinging eddies. With the development of more advanced assimilation methods and additional observations, future prediction systems should have increased accuracy in representing the three-dimensional ocean.

## Acknowledgements

This work was supported in part by a grant of computer time from the DOD high Performance Computing Modernization Program at the Navy DoD Supercomputing Resource Center. It was sponsored by the Office of Naval Research (ONR) through the NRL project Kuroshio and Ryukyu current dynamics in the western Pacific Ocean (61153 N). Current meter observation data south of Miyakojima and Okinawa were obtained from http://www.jamstec.go.jp/iorgc/ocorp/ktsfg/data/mooring/CM. The reanalysis output can be obtained from http://hycom.org. Comments and suggestions by Prof. Motoyoshi Ikeda and two anonymous reviewers are acknowledged.

## References

Andres, M., Park, J.-H., Wimbush, M., Zhu, X.-H., Chang, K.-I., Ichikawa, H., 2008. Study of the Kuroshio/Ryukyu current system based on satellite-altimeter and in situ measurements. Journal of Oceanography 64 (6), 937–950.

Bleck, R., 2002. An oceanic general circulation model framed in hybrid isopycnic-Cartesian coordinates. Ocean Modelling 4, 55–88.

Bloom, S.C., Takacs, L.L., daSilva, A.M., Ledvina, D., 1996. Data assimilation using incremental analysis updates. Monthly Weather Review 124, 1256–1271.

Crosby, D.S., Breaker, L.C., Gmmill, W.H., 1993. A proposed definition for vector correlation in geophysics. Journal of Atmospheric and Oceanic Technology 10, 355–367.

Cummings, J.A., Smedstad, O.M., 2013. Variational data assimilation for the global ocean. In: Park, S.K., Xu, L. (Eds.), Data Assimilation for Atmospheric, Oceanic and Hydrologic Applications, vol. II. Springer-Verlag, Berlin, Heidelberg, pp. 303–343.

Feng, M., Mitsudera, H., Yoshikawa, Y., 2000. Structure and variability of the Kuroshio in Tokara Strait. Journal of Physical Oceanography 30, 2257–2276.

Hurlburt, H.E., Metzger, E.J., Richman, J.G., Chassignet, E.P., Drillet, Y., Hecht, M.W., Le Galloudec, O., Shriver, J.F., Xu, X., Zamudio, L., 2011. Dynamical evaluation of ocean models using the Gulf Stream as an example. In: Schiller, A., Brassington, G.B. (Eds.), Operational Oceanography in the 21st Century. Springer Science Business Media B.V., pp. 545–609.

Ichikawa, H., Beardsley, R.C., 1993. Temporal and spatial variability of volume transport of the Kuroshio in the East China Sea. Deep-Sea Research Part I 40, 583–605.

Ichikawa, H., Nakamura, H., Nishina, A., Higashi, M., 2004. Variability of northeastward current southeast of northern Ryukyu Islands. Journal of Oceanography 60, 351–363.

Imawaki, S., Uchida, H., Ichikawa, H., Fukasawa, M., Umatani, S.ASUKA Group, 2001. Satellite altimeter monitoring the Kuroshio transport south of Japan. Geophysical Research Letters 28, 17–20.

Isobe, A., Imawaki, S., 2002. Annual variation of the Kuroshio transport in a two-layer numerical model with a ridge. Journal of Physical Oceanography 32, 994–1009.

Johns, W.E., Lee, T.N., Zhang, D., Zantopp, R., Liu, C.T., Yang, Y., 2001. The Kuroshio east of Taiwan: moored transport observations from the WOCE PCM-1 array. Journal of Physical Oceanography 31, 1031–1053.

Kamachi, M., Kuragano, T., Ichikawa, H., Nakamura, H., Nishina, A., Isobe, A., Ambe, D., Arai, M., Gohda, N., Sugimoto, S., Yoshita, K., Sakurai, T., Uboldi, F., 2004. Operational data assimilation system for the Kuroshio south of Japan: reanalysis and validation. Journal of Oceanography 60, 303–312.

Konda, M., Ichikawa, H., Han, I.-S., Zhu, X.-H., Ichikawa, K., 2005. Variability of current due to mesoscale eddies on the bottom slope southeast of Okinawa Island. Journal of Oceanography 61, 1089–1099.

Lee, T.N., Johns, W.E., Liu, C.T., Zhang, D., Zantopp, R., Yang, Y., 2001. Mean transport and seasonal cycle of the Kuroshio east of Taiwan with comparison to the Florida Current. Journal of Geophysical Research 106, 22143–22158.

Liu, Y., Yuan, Y., 2000. Variation of the currents east of the Ryukyu Islands in 1998. La Mer 38, 179–184.

Metzger, E.J., Smedstad, O.M., Thoppil, P.G., Hurlburt, H.E., Wallcraft, A.J., Franklin, D.S., Shriver, J.F., Smedstad, L.F., 2008. Validation Test Report for the Global Ocean Prediction System V 3.0 – 1/12° HYCOM/NCODA Phase I. NRL Memorandum Report NRL/MR/7320-08-9148, 85 pp.

Metzger, E.J., Smedstad, O.M., Thoppil, P.G., Hurlburt, H.E., Franklin, D.S., Peggion, G., Shriver, J.F., Wallcraft, A.J., 2010. Validation Test Report for the Global Ocean Prediction System V 3.0 – 1/12° HYCOM/NCODA Phase II. NRL Memorandum Report NRL/MR/7320-10-9236, 76 pp.

Metzger, E.J., Smedstad, O.M., Thoppil, P.G., Hurlburt, H.E., Cummings, J.A., Wallcraft, A.J., Zamudio, L., Franklin, D.S., Posey, P.G., Phelps, M.W., Hogan, P.J., Bub, F.L., Dehaan, C.J., 2014. US Navy operational global ocean and Arctic ice prediction systems, special issue on navy operational models. Oceanography 27 (3), 32–43.

Na, H., Wimbush, M., Park, J.-H., Nakamura, H., Nishina, A., 2014. Observations of flow variability through the Kerama Gap between the East China Sea and the Northwestern Pacific. Journal of Geophysical Research 119, 689–703. http://dx.doi.org/10.1002/2013JC008899.

Nagano, A., Ichikawa, H., Miura, T., Ichikawa, K., Konda, M., Yoshikawa, Y., Obama, K., Murakami, K., 2007. Current system east of the Ryukyu Islands. Journal of Geophysical Research 112. http://dx.doi.org/10.1029/2006JC003917.

Nagano, A., Ichikawa, H., Miura, T., Ichikawa, K., Konda, M., Yoshikawa, Y., Obama, K., Murakami, K., 2008. Reply to comment by Xie-Hua Zhu et al. on "Current system east of the Ryukyu Islands". Journal of Geophysical Research 113, C03021. http://dx.doi.org/10.1029/2007JC004561.

Nakamura, H., Ichikawa, H., Nishina, A., 2007. Numerical study of the dynamics of the Ryukyu Current system. Journal of Geophysical Research 112. http://dx.doi.org/10.1029/2006JC003595.

Nitani, H., 1972. Beginning of the Kuroshio. In: Stommel, H., Yoshida, K. (Eds.), Kuroshio: Its Physical Aspects. Univ. of Tokyo Press, Tokyo, pp. 129–163.

Ollitrault, M., Rannou, J.-P., 2013. ANDRO: an Argo based deep displacement dataset. Journal of Atmospheric and Oceanic Technology 30, 759–788. http://dx.doi.org/10.1175/JTECH-D-12-00073.1.

Saha, S. et al., 2010. The NCEP climate forecast system reanalysis. Bulletin of the American Meteorological Society 91. http://dx.doi.org/10.1175/2010BAMS3001.1.

Takikawa, T., Ichikawa, H., Ichikawa, K., Kawae, S., 2005. Extraordinary subsurface mesoscale eddy detected in the southeast of Okinawa in February 2002. Geophysical Research Letters 32, L17602. http://dx.doi.org/10.1029/2005GL023842.

Thoppil, P.G., Richman, J.G., Hogan, P.J., 2011. Energetics of a global ocean circulation model compared to observations. Geophysical Research Letters 38 (15), 607. http://dx.doi.org/10.1029/2011GL048347.

Worthington, L.V., Kawai, H., 1972. Comparison between deep sections across the Kuroshio and the Florida Current and Gulf Stream. In: Stommel, H., Yoshida, K. (Eds.), Kuroshio: Its Physical Aspects. Univ. of Tokyo Press, Tokyo, pp. 371–385.

You, S.H., Yoon, J.H., 2004. Modeling of the Ryukyu Current along the Pacific side of the Ryukyu Islands. Pacific Oceanography 2, 44–51.

You, S.H., Yoon, J.H., Kim, C.-H., 2009. Modeling and verification of the subsurface current core of the Ryukyu Current. Terrestrial, Atmospheric and Oceanic Sciences 20, 761–768.

Yu, Z., Metzger, E.J, Thoppil, P.G., Hurlburt, H.E., Zamudio, L., Smedstad, O.M., Na, H., Nakamura, H., Park, J.-H., 2015. Annual cycle of volume transport through Kerama Gap revealed by a 20-year global hybrid coordinate ocean model reanalysis. Ocean Modelling 96, 203–213.

Yuan, Y., Takano, K., Pan, Z., Su, J., Kawatate, K., Imawaki, S., Yu, H., Chen, H., Ichikawa, H., Umatani, S., 1994. The Kuroshio in the East China Sea and the currents east of the Ryukyu Islands during autumn 1991. La Mer 32, 235–244.

Zhang, D., Lee, T.N., Johns, W.E., Liu, C.T., Zantopp, R., 2001. The Kuroshio east of Taiwan: modes of variability and relationship to interior ocean mesoscale eddies. Journal of Physical Oceanography 31, 1054–1074.

Zhu, X.-H., Han, I.-S., Park, J.-H., Ichikawa, H., Murakami, K., Kaneko, A., Ostrovskii, A., 2003. The Northeastward Current southeast of Okinawa Island observed during November 2000 to August 2001. Geophysical Research Letters 30, 1071. http://dx.doi.org/10.1029/2002GL015867.

Zhu, X.-H., Ichikawa, H., Ichikawa, K., Takeuchi, K., 2004. Volume transport variability southeast of Okinawa Island estimated from satellite altimeter data. Journal of Oceanography 60, 953–962.

Zhu, X.-H., Park, J.-H., Kaneko, I., 2005. The Northeastward Current southeast of Okinawa Islands in late fall of 2000 estimated by an inverse technique. Geophysical Research Letters 32, L05608. http://dx.doi.org/10.1029/2004GL022135.

Zhu, X.-H., Park, J.-H., Kaneko, I., 2006. Velocity structures and transports of the Kuroshio and Ryukyu Current during fall of 2000 estimated by an inverse technique. Journal of Oceanography 62, 587–596.

Zhu, X.-H., Park, J.-H., Wimbush, W., Yang, C.-H., 2008. Comment on "Current system east of the Ryukyu Islands" by A. Nagano et al. Journal of Geophysical Research 113, C03020. http://dx.doi.org/10.1029/2007JC004458.

Zhu, X.-H., Huang, D.J., Guo, X.Y., 2010. Autumn intensification of the Ryukyu Current during 2003–2007. Science China Earth Sciences. http://dx.doi.org/10.1007/s11430-010-002202.